Analysis of cis-acting requirements of the Rh3 and Rh4 genes reveals a bipartite organization to rhodopsin promoters in Drosophila melanogaster.

M E Fortini and G M Rubin

Genes Dev. 1990 4: 444-463
Access the most recent version at doi:10.1101/gad.4.3.444

Analysis of *cis*-acting requirements of the *Rh3* and *Rh4* genes reveals a bipartite organization to rhodopsin promoters in *Drosophila melanogaster*

Mark E. Fortini and Gerald M. Rubin

Howard Hughes Medical Institute, Department of Molecular and Cell Biology, University of California, Berkeley, California 94720 USA

The rhodopsin genes of *Drosophila melanogaster* are expressed in nonoverlapping subsets of photoreceptor cells within the insect visual system. Two of these genes, *Rh3* and *Rh4*, are known to display complementary expression patterns in the UV-sensitive R7 photoreceptor cell population of the compound eye. In addition, we find that *Rh3* is expressed in a small group of paired R7 and R8 photoreceptor cells at the dorsal eye margin that are apparently specialized for the detection of polarized light. In this paper we present a detailed characterization of the *cis*-acting requirements of both *Rh3* and *Rh4*. Promoter deletion series demonstrate that small regulatory regions (<300 bp) of both R7 opsin genes contain DNA sequences sufficient to generate their respective expression patterns. Individual *cis*-acting elements were further identified by oligonucleotide-directed mutagenesis guided by interspecific sequence comparisons. Our results suggest that the *Drosophila* rhodopsin genes share a simple bipartite promoter structure, whereby the proximal region constitutes a functionally equivalent promoter "core" and the distal region determines cell-type specificity. The expression patterns of several hybrid rhodopsin promoters, in which all or part of the putative core regions have been replaced with the analogous regions of different rhodopsin promoters, provide additional evidence in support of this model.

[*Key Words*: *Drosophila*; compound eye; rhodopsin promoters; cell-type specific gene expression; oligonucleotide-directed mutagenesis; polarized light detection]

Received November 9, 1989; revised version accepted December 29, 1989.

Studies of mammalian transcription factors and their target promoter sequences suggest that eukaryotic gene regulation is achieved via combinatorial control mechanisms, whereby a modest number of regulatory factors interact with a much larger number of downstream genes (for review, see Dynan 1989; Mitchell and Tjian 1989). Exactly how particular combinations of transcription factors are used to generate strikingly different temporal and spatial patterns of gene expression, however, is still poorly understood. We have performed a systematic analysis of the rhodopsin gene promoters of *Drosophila melanogaster* in the hope of elucidating an underlying logic to combinatorial control in transcription. In contrast to other well-characterized *Drosophila* genes, which are generally regulated at the level of whole tissues or organs (discussed in Fischer and Maniatis 1988), the four rhodopsin genes isolated to date are expressed with exquisite specificity in different photoreceptor cell subpopulations of the *Drosophila* larval and adult visual systems. Our investigations have concentrated primarily on patterns of rhodopsin gene expression within the adult visual system, which consists of the compound eyes and ocelli. The ocelli are three small light-sensing organs located on the vertex of the adult head.

The photoreceptor cells of the *Drosophila* adult comprise a small set of well-defined cell types (Fig. 1). The compound eye, itself, consists of a repetitive hexagonal array of ~700 unit eyes or ommatidia, each containing a regular trapezoidal array of eight photoreceptor cells (Ready et al. 1976). Spectral, morphological, and genetic criteria divide the eight ommatidial photoreceptors into three distinct cell types: cells R1–R6, cell R7, and cell R8 (Harris et al. 1976; Heisenberg and Wolf 1984). These three cell types differ from each other with respect to the positions of their rhabdomeres within the ommatidium, their axonal projection patterns to the optic lobes, their spectral sensitivities, and their specific absence or degeneration in certain mutants. By the same criteria, the ~90 photoreceptor cells associated with each ocellus comprise a fourth class of adult photoreceptor cell type (Schmidt 1975; Hu et al. 1978; Stark et al. 1989).

The different properties of the adult photoreceptor cell types extend to their pattern of rhodopsin gene expression. *Rh1* is expressed only in the outer photoreceptors R1–R6, *Rh2* is expressed only in the ocellar photoreceptors, and *Rh3* and *Rh4* are expressed in nonoverlapping subsets of the R7 photoreceptor cell population (Mismer and Rubin 1987; Montell et al. 1987; Mismer et al. 1988; Pollock and Benzer 1988). Three of these rho-

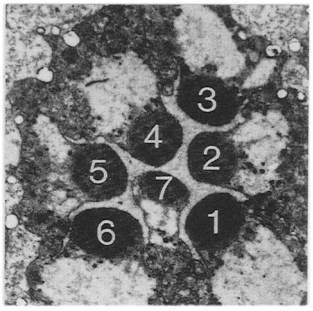

Photoreceptor cell type	Rhabdomere location	Synaptic ganglion	Spectral sensitivity	Rhodopsin	Specific mutation
R1-6	peripheral	lamina	blue	*Rh1* (*ninaE*)	*ora, rdgB*
R7	central-distal	medulla I	UV	*Rh3, Rh4*	*sev, boss*
R8	central-proximal	medulla II	blue-green	?	?
ocellar photoreceptors	ocelli	ocellar ganglion	short blue	*Rh2*	*oc, noc*

Figure 1. Summary of the four major photoreceptor cell types in *D. melanogaster*. (*Left*) Tangential EM section through the distal portion of the retina showing the trapezoidal arrangement of photoreceptor cell rhabdomeres within a single ommatidium (micrograph courtesy of A. Tomlinson). Photoreceptor cells R1–7 are numbered according to Dietrich (1909). The R8 cell rhabdomere is located beneath that of the R7 cell, and the R8 cell body is positioned between R1 and R2. (*Right*) The morphological, spectral, and genetic criteria distinguishing each photoreceptor cell type.

dopsins, namely *Rh1*, *Rh3*, and *Rh4*, are also expressed in the larval photoreceptor organs (Mismer and Rubin 1987; Pollock and Benzer 1988). Extensive study of the analogous visual systems of *Musca domestica* and *Calliphora erythrocephala* (for review, see Hardie 1985, 1986) suggests that the four *Drosophila* rhodopsin genes isolated so far can account for all visual pigment deposition in three of the four *Drosophila* adult photoreceptor cell types, namely the R1–R6, R7, and ocellar photoreceptors. Spectral properties of the R8 cells in these larger dipterans indicate that two rhodopsin genes expressed in nonoverlapping R8 subpopulations of the *Drosophila* retina have yet to be identified.

Previous analysis of the regulatory regions of the *Rh1* and *Rh2* genes has shown that their expression in particular photoreceptor cell types is transcriptionally mediated and that small promoter regions contain all of the required *cis*-acting elements for their respective patterns (Mismer and Rubin 1987; Mismer et al. 1988). This report concerns the *cis*-acting requirements of the two R7-specific rhodopsin genes *Rh3* and *Rh4*. We show that the expression of these two genes in nonoverlapping photoreceptor R7 subpopulations is transcriptionally mediated by promoter regions <300 bp in length. Promoter fusions of these two genes to the bacterial reporter gene *lacZ* were used to clarify previously obscure details of their expression patterns, allowing each of the *Drosophila* R7 opsins to be assigned as the functional homolog of one of the two R7 opsins of *Musca* and *Calliphora*. The promoter regions of all four rhodopsin gene homologs of *Drosophila virilis* were isolated and sequenced to identify potentially conserved *cis*-acting elements. In addition, we have found that the *D. virilis Rh3* and *Rh4* promoters direct R7-specific gene expression when introduced into the *D. melanogaster* genome. Oligonucleotide-directed mutagenesis of the R7 opsin promoters, guided by cross-species sequence homologies, has identified several functional *cis*-acting elements for these two promoters. The results of these experiments lead us to propose that the proximal region of each rhodopsin promoter constitutes an interchangeable promoter "core," with cell-type specificity determined by upstream sequences unique to each promoter. Additional support for this model is furnished by the expression patterns of several hybrid promoter constructs that combine the core and the cell-type specificity regions of two different rhodopsin promoters.

Results

Reconstitution of Drosophila *R7-specific opsin expression patterns using* Rh3–lacZ *and* Rh4–lacZ *fusions*

RNA blot analysis has previously shown that in the adult, *Rh4* is expressed exclusively in R7 photoreceptor cells and *Rh3* is expressed predominantly in R7 cells (Fryxell and Meyerowitz 1987; Montell et al. 1987; Zuker et al. 1987). *Rh3* transcripts were also detected at lower abundance in *sevenless* (*sev*) heads, which lack all R7 photoreceptors, and at trace levels in adult body tissues. The non-R7 cell expression of *Rh3* was not localized further. In situ hybridization of gene-specific *Rh3* and *Rh4* probes to serial tissue sections of the adult retina has demonstrated that these two genes are expressed in nonoverlapping R7 cell subpopulations (Montell et al. 1987). As a first step toward a systematic analysis of the regulatory regions of *Rh3* and *Rh4*, putative promoter sequences were fused to the bacterial reporter gene *lacZ* (encoding β-galactosidase) and introduced into *D. melanogaster* by P-element-mediated germ line transformation. These constructs were made with two goals in mind: (1) to refine our understanding of the wild-type *Rh3* and *Rh4* expression patterns, especially by localizing the *Rh3* expression detected in *sev* heads, and (2) to define large promoter fragments that confer every feature of the endogenous *Rh3* and *Rh4* expression patterns on a bacterial reporter gene.

Two independent transformants of an *Rh3–lacZ* fusion containing a −2.6-kb to +18-bp promoter fragment were obtained, where +1 denotes the start site of transcription. These transformants, termed P[*Rh3.2600lacZ*]1 and P[*Rh3.2600lacZ*]2, were analyzed by histochemical staining with the chromogenic substrate X-gal (see Materials and methods). Within the retina, both

P[*Rh3.2600lacZ*] lines exhibit staining of individual R7 photoreceptors, as judged by their characteristic morphology and localization to the distal half of the retina (Fig. 2A). Throughout most of the retinal field, ~30% of the R7 cells are stained in an apparently stochastic distribution pattern. The presence of unstained R7 cells in the P[*Rh3.2600lacZ*] retinas was confirmed by double staining of semithin tissue sections with X-gal and Hoechst dye (Fig. 2B). The Hoechst dye labels all nuclei and reveals that only a subset of nuclei in the R7 nuclear layer, which is located in the apical portion of the retina just beneath the R1–R6 nuclear layer, corresponds to R7 cell bodies expressing the *Rh3–lacZ* fusion.

The histochemical staining observed for P[*Rh3.2600lacZ*] within the retina corresponds closely to the distribution of endogenous *Rh3* transcripts as determined by in situ hybridization (Zuker et al. 1987). Unlike the rhodopsin mRNA, however, the β-galactosidase enzyme diffuses throughout the length of the photoreceptor neuron, allowing the axonal morphology of *Rh3*-expressing R7 photoreceptors to be visualized. With long staining times, it is possible to follow the thread-like axonal projections of these cells as they emerge from the R7 cell bodies, traverse the proximal retina and the lamina, cross over each other at the optic chiasma, and enter the medulla to make their synaptic connections with second-order neurons (similar to Fig. 2J). The precisely aligned synaptic terminals of these axons at a single layer of the medulla are especially evident, as is their characteristic swelling prior to entering this optic ganglion (Fig. 2A,F). Within the medulla neuropil, the stained axonal terminals of *Rh3*-expressing R7 cells form a broken line punctuated by gaps that presumably reflect the presence of unstained synaptic terminals of *Rh4*-expressing R7 photoreceptor neurons. The axonal staining in the medulla observed for P[*Rh3.2600lacZ*] is in marked contrast to transformants bearing *Rh1–lacZ* fusions, which display staining only in the lamina, where R1–R6 photoreceptor axons terminate (Mismer and Rubin 1987).

Although most of the retina of these *Rh3–lacZ* transformants exhibits staining of an apparently random sub-

Figure 2. Histochemical analysis of *Rh3–lacZ* and *Rh4–lacZ* transformant lines. Cryostat sections (10–14 μm) of head tissues were prepared and stained as described in Materials and methods. (*A*) Horizontal section through the compound eye and optic lobes of the transformant line P[*Rh3.2600lacZ*]1, showing staining of ~30% of the R7 cell bodies in the distal retina (re) and their synaptic terminals in the medulla (me). (la) Lamina; (oc) optic chiasma. (*B*) Higher magnification view of a P[*Rh3.2600lacZ*]1 retina counterstained with Hoechst, demonstrating R7 nuclei corresponding to unstained R7 cells. Note the two unstained R7 cell nuclei indicated by the solid arrowheads flanking the nucleus of a stained R7 cell. The right-most portion shows the most apical region of the retina, which contains nuclei of R1–R6 cells, pigment cells, and cone cells. The R7 nuclei are located just beneath this dense nuclear layer, and the R8 nuclei are located in the basal region of the retina (left-most portion). (*C*) Sagittal section through a P[*Rh3.2600lacZ*]2 retina demonstrating *Rh3–lacZ* expression in paired R7 and R8 photoreceptors at the dorsal margin (between solid arrows; dorsal at top, anterior to the left). (*D*) Frontal section through the dorsal eye margin of P[*Rh3.2600lacZ*]1 (dorsal at top), showing stained dorsal marginal photoreceptors (between solid arrows). (*E*) Frontal section through the dorsal eye margin of P[*Rh3.2600lacZ*]1 at a deeper level than in *D*, counterstained with Hoechst (orientation as in *D*). Because of the curvature of the eye, the line of stained dorsal marginal R8 cells (between open arrows) is interrupted by a region of R8 nuclei corresponding to unstained, nonmarginal R8 cells. Synaptic terminals of dorsal marginal central photoreceptors display pronounced staining in the dorsal medulla in such sections (small solid arrow). Stained nonmarginal R7 photoreceptors are present in the region between the large solid arrows. (*F*) Horizontal section through a P[*Rh3.2600lacZ*]1 dorsal medulla showing dorsal marginal R7 and R8 synaptic terminals at the periphery of this optic lobe (circled terminals), as well as staining of a random subset (~30%) of nonperipheral R7 synaptic terminals. Additional staining on the right is attributable to central photoreceptor axons swelling prior to entering the medulla. (*Inset*) An expanded view of the posterior (bottom of *F*) set of circled dorsal marginal synaptic terminals. The two dorsal marginal R8 terminals (open arrows) make synaptic connections at a slightly more shallow level of the medulla than that of the dorsal marginal R7 terminals (solid arrows). (*G*) Sagittal section through the dorsal marginal retina of sev^{d2}; P[*Rh3.2600lacZ*]2, showing stained R8 cells (cf. *C*; same orientation). (*H*) Frontal section through a sev^{d2}; P[*Rh3.2600lacZ*]1 retina at same level and orientation as in *D*. Staining is only observed in dorsal marginal R8 cells. (*I*) Sagittal section through dorsal head tissues of sev^{d2}; P[*Rh3.2600lacZ*]1. Axonal projections of stained dorsal marginal R8 cells in the retina (re) extend through the lamina (la), and terminate in the two dorsal-most rows of the medulla neuropil (me), as indicated by the solid arrowheads. The regularly spaced dots of staining at the lamina–medulla interface are additional dorsal marginal R8 axons passing through the plane of the section near the optic chiasma (dorsal at top, anterior to the right). (*J*) Horizontal section through P[*Rh4.1900lacZ*]5 head tissues, counterstained with Hoechst. With long staining times, the thin axonal fibers of individual R7 cells are visible as they traverse the proximal retina and the lamina on their way to the medulla. (*K*) Higher magnification view of a P[*Rh4.1900lacZ*]5 retina counterstained with Hoechst, confirming the presence of unstained R7 cells and their nuclei (solid arrowheads; orientation as in *B*). (*L*) Sagittal section through P[*Rh4.1900lacZ*]5 head tissues. Note that although the majority of R7 cells and their synaptic terminals are stained, the dorsal marginal retina and its corresponding medulla neuropil are devoid of staining (regions between solid arrowheads; cf. *C*, *E*, *F*, *G*, and *I*). (*M*) Tangential section through the distal retina of P[*Rh4.1900lacZ*]5, showing that a stochastically distributed majority of the ommatidia contain stained R7 cells. Because of the curvature of the eye, the central area of this section passes through the proximal retina, which contains R8 instead of R7 cell bodies and hence shows little staining (dorsal at top, anterior to the right). (*N*) Horizontal section through a P[*Rh4.1900lacZ*]2 medulla, displaying an abundance (~70%) of stained synaptic terminals complementary to that observed for the typical P[*Rh3.2600lacZ*] medulla shown in *F*. (*O*) Horizontal section of P[*Rh3.2600lacZ*]1/P[*Rh4.1900lacZ*]2 compound eye and optic lobe structures, displaying staining of all R7 cells and their synaptic terminals. (*P*) Scanning EM photograph of a wild-type *D. melanogaster* compound eye (courtesy of B. Kimmel). Specialized dorsal marginal R7 and R8 photoreceptors are present in a single row of ommatidia adjacent to and extending along the dorsal head cuticle, as indicated by open arrows.

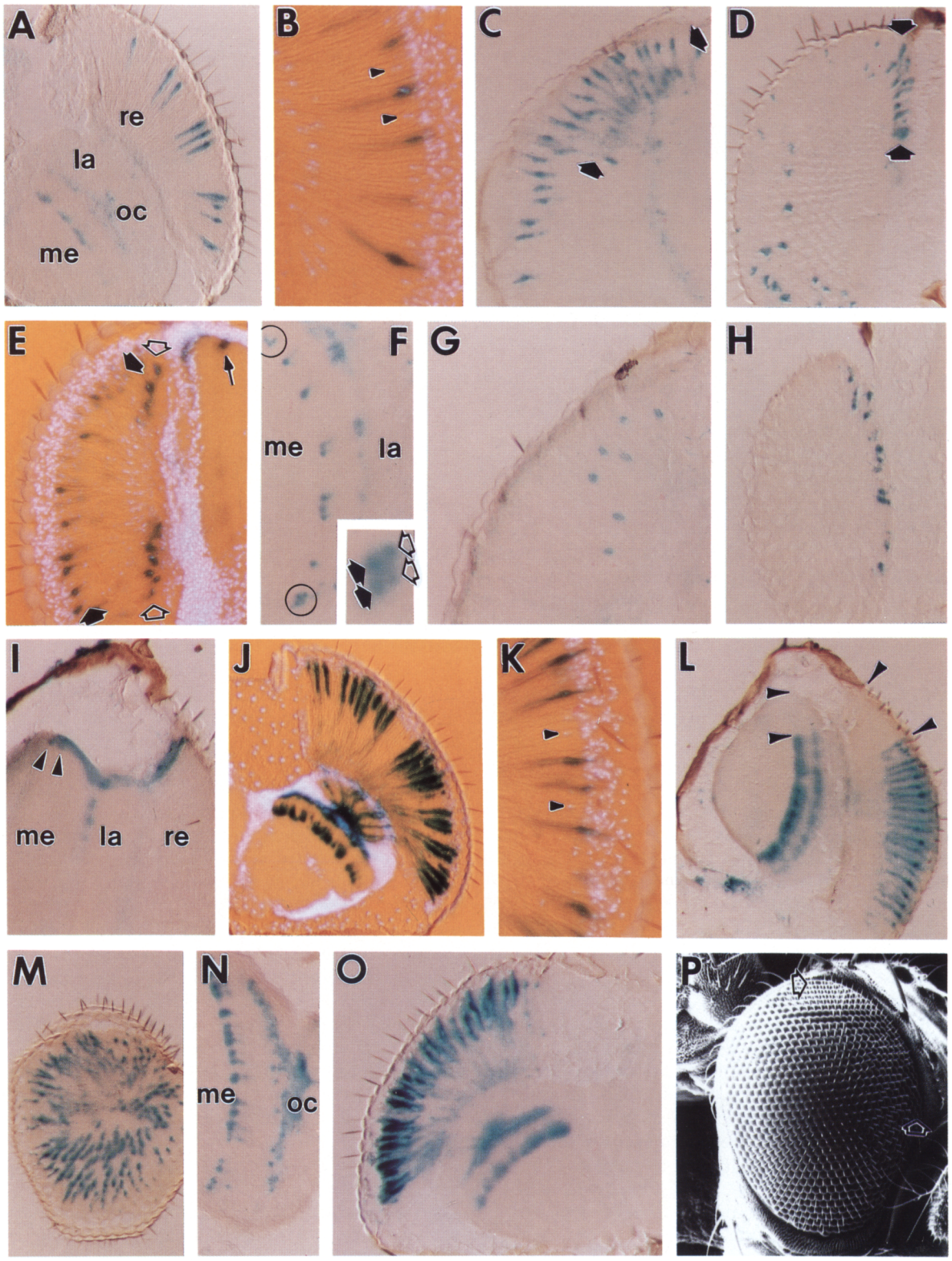

Figure 2. {*See facing page for legend.*}

population of ~30% of the R7 photoreceptors, the dorsal marginal region of the retina shows a strikingly nonrandom pattern of staining. A single row of ~25 ommatidia along the extreme dorsal anterior eye margin, adjoining the head cuticle of the vertex and frons, exhibits staining of all R7 and R8 photoreceptor cell pairs (Fig. 2C,D,E,P). The presence of reporter gene activity in dorsal marginal R8 cells was confirmed by histochemical analysis of P[*Rh3.2600lacZ*] in a sev^{d2} genetic background. To ensure that the sev^{d2} phenotype is fully penetrant in the dorsal marginal ommatidia, eyes of these individuals were examined by antidromic illumination after optical neutralization of the cornea (Franceschini and Kirschfeld 1971a,b) prior to sectioning and staining. As expected, flies of genotype sev^{d2}; P[*Rh3.2600lacZ*] display staining only in the dorsal marginal R8 cells and in no other region of the retina (Fig. 2G–I). This finding, together with the number of *Rh3*-expressing R7 cells throughout the entire retina, indicates that these specialized R8 cells could account for the *Rh3* transcription previously detected in *sev* heads. Examination of serial sections of P[*Rh3.2600lacZ*] in both wild-type and sev^{d2} genetic backgrounds reveals that after passing through the optic chiasma, the axonal projections of these dorsal marginal cells terminate in the two most peripheral synaptic rows extending along the dorsal posterior neuropil of the medulla (Fig. 2E,F,I). These synaptic terminals generally exhibit more pronounced staining than those of nonmarginal *Rh3*-expressing R7 cells present in the same preparation (Fig. 2E). We were unable to localize the body expression of *Rh3* detected previously (Montell et al. 1987) using P[*Rh3.2600lacZ*] because of high levels of endogenous β-galactosidase activity in many body tissues.

An analogous histochemical study was performed for *Rh4*, utilizing a −1.9-kb to +7-bp promoter fragment fused to *lacZ*. Eleven independent transformant lines were analyzed in a wild-type genetic background. As with the *Rh3–lacZ* fusion, this *Rh4–lacZ* construct labels a subpopulation of R7 photoreceptor cell bodies, their axonal projections, and their synaptic terminals in the medulla (Fig. 2J,L–N). The P[*Rh4.1900lacZ*] lines, however, stain ~70% of the total photoreceptor R7 cell population in an apparently random distribution across the retina, as confirmed by X-gal/Hoechst double staining (Fig. 2K). Several of the *Rh4–lacZ* transformant lines were also analyzed in a sev^{d2} genetic background, and no staining was detected (data not shown).

A previous in situ hybridization study using *Rh3* and *Rh4* gene-specific probes has demonstrated that these two genes are expressed in complementary subsets of R7 cells within a small sampled region of ~40 ommatidia (Montell et al. 1987). Our histological analysis of *Rh3–lacZ* and *Rh4–lacZ* expression over the entire retinal field is consistent with this pattern. As expected, double transformants of genotype P[*Rh3.2600lacZ*]1/P[*Rh4.1900lacZ*]2 display staining of all R7 cell bodies and synaptic terminals (Fig. 2O). Furthermore, examination of serial sections of P[*Rh4.1900lacZ*] reveals that although the majority of R7 cells across the surface of the retina are stained, the *Rh3*-specific dorsal marginal region of the eye and the corresponding region of the dorsal medulla neuropil are devoid of staining (Fig. 2L).

Determination of minimal R7 opsin regulatory regions by promoter deletion analysis

The *Rh3–lacZ* and *Rh4–lacZ* analysis described above has defined large (>2000 bp) promoter fragments able to confer apparently wild-type opsin gene expression patterns on a bacterial reporter gene. Extensive 5′-deletion analysis of each of these fragments was next undertaken to identify the smallest functional promoter region for both *Rh3* and *Rh4*. The bacterial reporter gene *chloramphenicol acetyltransferase* (*CAT*) was chosen instead of *lacZ* for the deletion analysis to take advantage of the higher transformation efficiencies and sensitive quantitative assays available for this reporter gene. Although good histochemical assays are not available for the CAT enzyme, localization of promoter activity to R7 cells is easily monitored in transformant lines by simply measuring CAT activity in wild-type heads versus *sev* heads (for autosomal inserts) or *bride of sevenless (boss)* heads (for X-linked inserts).

Eight independent transformant lines of a 2.6-kb *Rh3* promoter–*CAT* fusion yield a CAT activity profile in wild-type and sev^{d2} or $boss^{3991}$ adult heads consistent with the *Rh3–lacZ* staining pattern as well as the endogenous *Rh3* expression pattern (P[*Rh3.2600CAT*]1–8; Fig. 3A). Approximately 90% of the CAT activity in these lines is localized to the R7 photoreceptor cells; the remaining 10% presumably reflects *Rh3* expression in dorsal marginal R8 cells. Some lines also show low but detectable CAT activity in body tissues, again consistent with the native *Rh3* transcript distribution. CAT activity was observed in dissected thoracic and abdominal tissues of these lines, indicating that *Rh3* body expression is not highly localized to a specific tissue or group of cells (data not shown). One line, P[*Rh3.2600CAT*]4, exhibits unusually high CAT activity in both the body and the head, although the proper cell-type specificity is preserved within the photoreceptors. The behavior of this line typifies the occasional position effect associated with P-element-mediated germ line transformation (Spradling and Rubin 1983; Hazelrigg et al. 1984; Levis et al. 1985).

Deletions of this full-length *Rh3* promoter fragment to −945, −583, −343, and −247 bp upstream of the transcriptional start site do not significantly affect any aspect of promoter function in this assay (Fig. 3A). Further deletion to −137 bp leads to a slight (two- to threefold) decrease in wild-type expression and the complete loss of dorsal marginal R8 expression in 12 of 14 lines examined (<0.1% of reference value in sev^{d2} or $boss^{3991}$ head samples; see P[*Rh3.137CAT*]1–14; Fig. 3A). Deletion of the *Rh3* promoter to −99 bp completely abolishes expression in four of seven transformant lines. The remaining three lines of this construct exhibit low to moderate CAT activity levels localized to the R7 cells (P[*Rh3.99CAT*]2, 4, and 5; Fig. 3A). Further deletion of

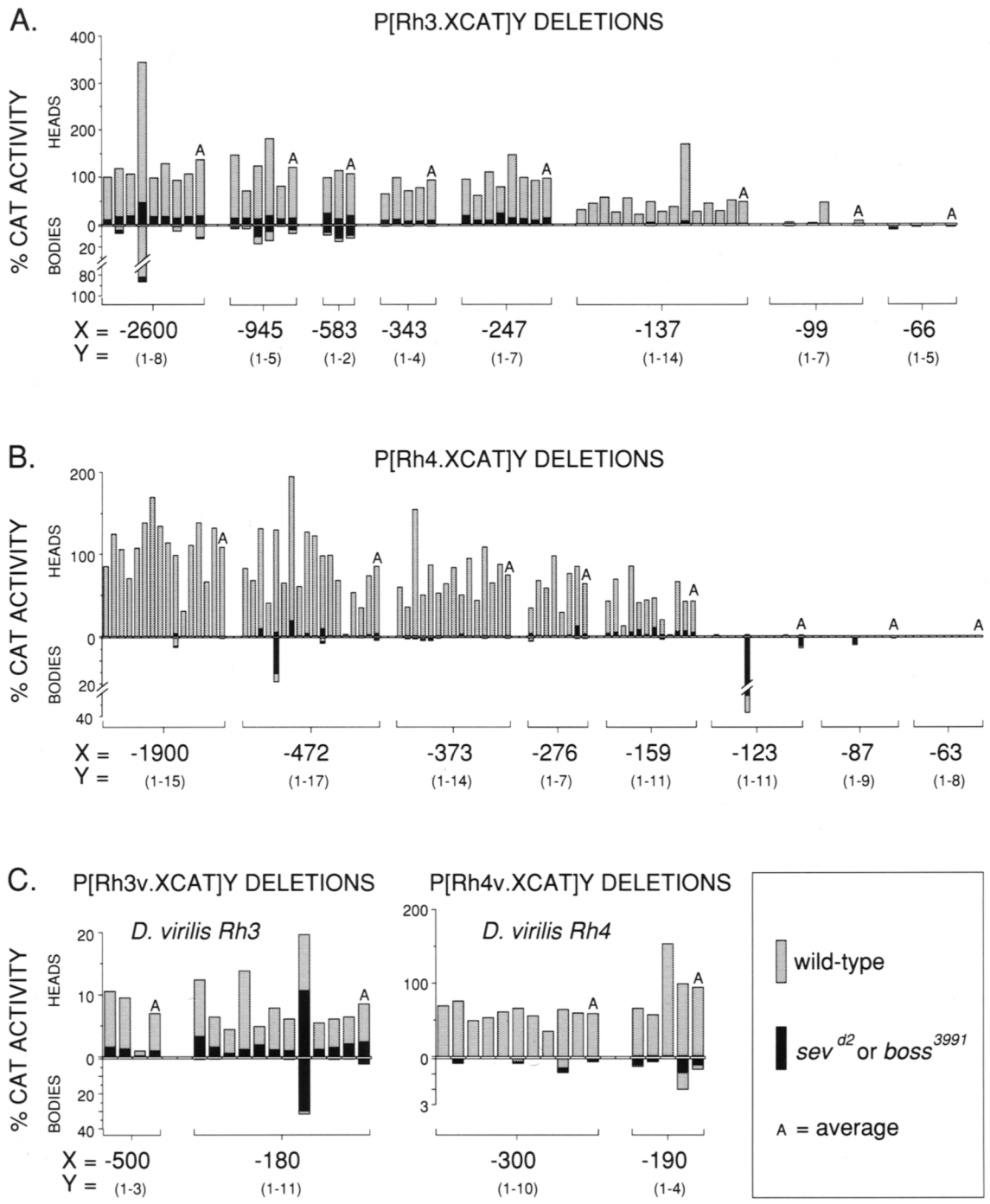

Figure 3. Histograms summarizing the deletion analysis of the *D. melanogaster Rh3* promoter (*A*), the *D. melanogaster Rh4* promoter (*B*), and the *D. virilis Rh3* and *Rh4* promoters (*C*). CAT assays were performed as described in Materials and methods. Each position along the axis of the abscissa represents a single transformant line, with head CAT activity levels plotted above the axis and body CAT activity levels plotted below the axis. CAT activity levels measured in wild-type tissues are shown as shaded bars; solid bars show the amount present in *sev*^{d2} tissues (for autosomal insertions) or *boss*^{3991} tissues (for X-linked insertions). Each bar represents the average of at least two CAT assays on five heads or bodies of a given transformant line; error is estimated to be not greater than 15%. If no bar is present, CAT activity was <0.1% for that sample. All independent tranformant lines of a single construct, followed by their average CAT activity profile (A), are enclosed within the underlying bracket. Each bracket is labeled with information corresponding to the name of the transformant lines, where *X* is the number of nucleotides upstream of the transcriptional start site present in each promoter fragment (5′-deletion end point) and *Y* is the numerical designation of each transformant line (in the same order as in the histograms). CAT activity levels of all transformant lines here and in Fig. 5 are normalized to the wild-type head value of the standard reference line P[*Rh3.2600CAT*]1 (100%; the first hatched bar of *A*).

the *Rh3* promoter to −66 bp eliminates retinal expression (P[*Rh3.66CAT*]1–5; Fig. 3A).

As with *Rh3*, the large *Rh4* promoter fragment extending from −1.9 kb to +7 bp drives *CAT* expression in a manner consistent with both the endogenous *Rh4* transcriptional profile and the *Rh4–lacZ* staining pattern. Discounting minor position effects, fifteen independent transformant lines of P[*Rh4.1900CAT*] show CAT activity localized exclusively to the R7 photoreceptor cells (P[*Rh4.1900CAT*]1–15; Fig. 3B). The CAT activity levels detected among the different lines are fairly uniform and are quantitatively comparable to those measured in genetically wild-type *Rh3–CAT* transformant lines. Deletions of the *Rh4* promoter to −472, −373, and −276 bp do not appreciably impair either the strength or cell-type specificity of this promoter (Fig. 3B). Further deletion to −159 bp has two effects, suggesting that *Rh4* promoter function has now been perturbed slightly (P[*Rh4.159CAT*]1–11; Fig. 3B). First, the 11 independent transformant lines of this deletion construct display relatively high variation in wild-type head CAT activity. Second, CAT activity is detected in sev^{d2} and $boss^{3991}$ heads of these transformants, demonstrating a partial disruption of the stringent R7 cell specificity obtained with larger *Rh4* promoter constructs. Both of these effects may reflect the increased sensitivity of a crippled promoter to the regulatory properties of neighboring genomic sequences at its site of insertion. Further deletions of the *Rh4* promoter to −123, −87, and −63 bp completely eliminate retinal expression of the *Rh4–CAT* fusion genes (Fig. 3B).

This deletion analysis shows that for both *Rh3* and *Rh4*, proper cell-type-specific gene expression may be generated by sequences residing in a very small regulatory region. An *Rh3* promoter fragment from −247 to +18 bp and an *Rh4* fragment from −276 to +7 bp appear to contain all the *cis*-acting information needed to reproduce fully the wild-type R7 opsin gene expression patterns. Moreover, deletion of either of these small promoters by an additional 100 bp still fails to undermine seriously their basic specificity for the R7 photoreceptor cell type.

Isolation, sequencing, and functional characterization of D. virilis *rhodopsin promoters*

Having defined very small functional promoters for both *Rh3* and *Rh4*, we sought to identify the discrete *cis*-acting elements responsible for the regulatory properties of these small promoter regions. Systematic mutagenesis of all nucleotides from −119 to −2 bp of the *Rh1* promoter has proved to be an informative but laborious method for locating important *cis*-acting elements (Mismer and Rubin 1989). Instead, we have searched for putative *cis*-acting elements of the *D. melanogaster* rhodopsin genes by comparing the DNA sequences of their promoters to the corresponding promoter regions of the distantly related species *D. virilis*. This approach has proved quite effective in the analysis of regulatory domains of the *Drosophila* dopa decarboxylase gene (*Ddc*; Scholnick et al. 1986).

The *Rh1–4* homologs of *D. virilis* were isolated from a *D. virilis* genomic library using the corresponding *D. melanogaster* probes, as described in Materials and methods. DNA sequence was obtained for ~250 bp of the *D. virilis Rh1* promoter, ~260 bp of the *D. virilis Rh2* promoter, ~500 bp of the *D. virilis Rh3* promoter, and ~300 bp of the *D. virilis Rh4* promoter. Complete DNA sequence was also obtained for a *D. melanogaster Rh3* promoter fragment extending to −1039 bp and a *D. melanogaster Rh4* promoter fragment extending to −472 bp. Pairwise homology searches among the eight rhodopsin gene promoters were performed in all possible combinations. As shown in Figure 4, most short stretches of high sequence similarity are clustered within the 150 bp immediately upstream of the transcriptional start site of each promoter.

To test whether the conserved DNA sequences reflect an actual conservation of promoter function, small putative promoter regions of the *D. virilis Rh3* and *Rh4* genes were fused to the *CAT* reporter module, introduced into *D. melanogaster*, and assayed for promoter function in wild-type and sev^{d2} or $boss^{3991}$ genetic backgrounds. For the *D. virilis Rh3* gene, promoter fragments of 500 and 180 bp confer a largely R7-specific expression pattern on the reporter gene (Fig. 3C). These 3 P[*Rh3v.500CAT*] and 11 P[*Rh3v.180CAT*] transformant lines display considerable quantitative variation in their wild-type levels of expression, which generally range from 5% to 20% of the wild-type levels measured for *D. melanogaster* nondeleted *Rh3–CAT* constructs. Expression of the *D. virilis* constructs is reduced approximately 10-fold in sev^{d2} or $boss^{3991}$ heads, reminiscent of the 10% contribution of the dorsal marginal R8 cells to the overall level of *D. melanogaster Rh3* retinal expression. The possibility that the small *D. virilis Rh3* promoters are active in the specialized dorsal marginal R7 and R8 photoreceptors has not been examined further. *D. virilis Rh4* promoter fragments of 300 and 190 bp confer a completely R7-specific expression pattern on the *CAT* reporter module at levels comparable to those of *D. melanogaster Rh4–CAT* constructs (Fig. 3C). The analysis of these *D. virilis Rh3–CAT* and *Rh4–CAT* transformant lines demonstrates that small *D. virilis* promoters interact functionally with the *D. melanogaster* transcriptional machinery to generate R7-specific patterns of gene expression.

Oligonucleotide-directed mutagenesis of the R7-specific opsin gene promoters

The finding that the *Rh3* and *Rh4* promoters of *D. virilis* are active in the *D. melanogaster* compound eye in an R7-specific manner argues that the evolutionarily conserved sequences of the R7 opsin promoters are strong candidates for *cis*-acting regulatory elements. This assertion is supported by the fact that exhaustive mutagenesis of the *D. melanogaster Rh1* proximal promoter region (Mismer and Rubin 1989) has failed to discover any functional *cis*-acting elements outside of a small region consisting of two sequences conserved in the *D. virilis Rh1* promoter and the four nucleotides separating

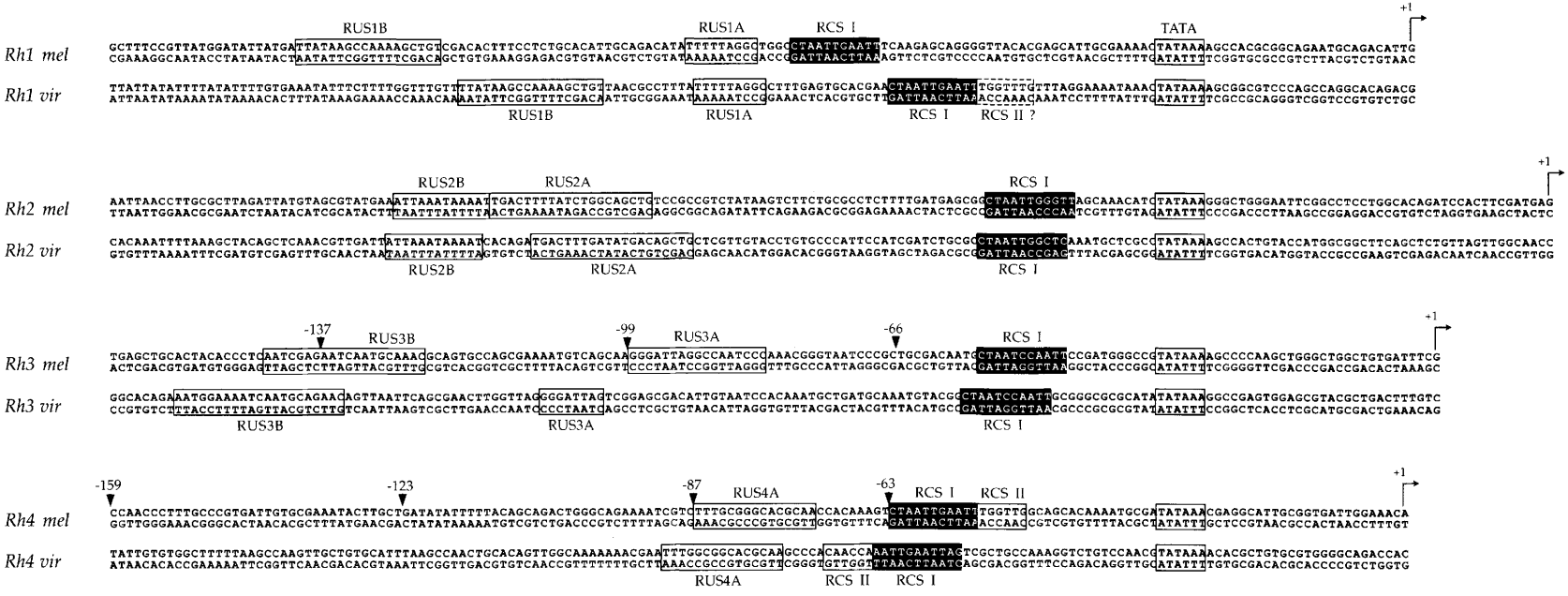

Figure 4. Sequence homologies detected among the rhodopsin promoters of *D. melanogaster* and *D. virilis*. All possible pairwise homology searches were performed among the eight available rhodopsin promoters, as described in the text. Evolutionarily conserved sequences clustered in the more proximal promoter regions are presented here. Additional homologies detected in the distal enhancers of the *D. melanogaster* and *D. virilis Rh1* promoters (M. Fuchs and G.M. Rubin, unpubl.) and in nonessential upstream regions of the *Rh3* and *Rh4* promoters of both species are not shown. Promoter sequences are aligned at the TATA box and the transcriptional start sites of the *D. melanogaster* promoters are indicated (+1). Putative *cis*-acting elements are labeled as in the text. For *Rh1*, the previously defined box A and box B elements (Mismer and Rubin 1989) have been renamed RUS1A and RCS I, respectively. RCS I elements are enclosed in solid boxes; other elements, including RCS II, the TATA box, and distal conserved sequences specific to each promoter type (RUS elements) are enclosed in open boxes. A sequence closely resembling RCS II is located adjacent to RCS I in the *D. virilis Rh1* promoter and is indicated by dashed lines. The relevance of this sequence, if any, for proper *D. virilis Rh1* expression has not been examined. For *D. melanogaster Rh3* and *Rh4*, the 5′-deletion end points of several of the promoter–*CAT* fusions analyzed in Fig. 3 are indicated above the sequence (solid arrowheads). The sources of these promoter sequences are as follows: *Rh1 mel* (Mismer and Rubin 1987), *Rh1 vir* (M. Fuchs, D. Schneider, and G.M. Rubin, unpubl.), *Rh2 mel* (Mismer et al. 1988), *Rh2 vir* (this study), *Rh3 mel* (this study; Fryxell and Meyerowitz 1987; Zuker et al. 1987), *Rh3 vir*, *Rh4 mel*, and *Rh4 vir* (this study).

them (RUS1A and RCS I; Fig. 4). For these reasons, cross-species sequence homologies were used as a guide in further investigations of the role of individual *cis*-acting elements in the *Rh3* and *Rh4* promoters of *D. melanogaster*.

Oligonucleotide-directed mutagenesis was used to alter each individual conserved sequence of the *D. melanogaster Rh3* gene. Several nonconserved regions were also altered to assess directly the validity of this targeted mutagenesis approach. In general, the mutagenesis was designed to maximize the number of mismatched nucleotides between wild-type and mutant sequences of a given region without affecting the nucleotide composition of the region. For *Rh3*, mutagenesis was performed on the promoter fragment extending from −343 to +18 bp. To ensure that this small promoter is truly wild-type for all features of the *Rh3* expression pattern, it was fused to *lacZ* and analyzed histochemically in transformed flies. Two independent transformants of P[*Rh3.343lacZ*] display staining of a stochastic subpopulation of R7 photoreceptor cells, as well as all dorsal marginal R7 and R8 cells, exactly as described for transformants of the 2.6-kb *Rh3* promoter–*lacZ* fusion gene (data not shown).

Mutagenesis of each of the three conserved regions of the *Rh3* promoter reveals that two are required for proper promoter function. Mutation of the *Rh3* rhodopsin core sequence I (RCS I; Fig. 4), an element common to each of the four rhodopsin promoters of both *D. melanogaster* and *D. virilis*, virtually destroys *Rh3* promoter function (P[*Rh3.343m8CAT*]1–6; Fig. 5A). The more distal *Rh3*-specific conserved sequence, termed RUS3B (rhodopsin upstream sequence B of *Rh3*), exhibits extraordinarily high promoter activity in body tissues when mutated (P[*Rh3.343m1CAT*]1–6; Fig. 5A). Mutation of the more proximal *Rh3*-specific conserved element RUS3A has little or no effect on the expression pattern of the *Rh3* promoter in this assay (P[*Rh3.343m5CAT*]1-15; Fig. 5A). The failure of this mutation to alter *Rh3* promoter function is surprising, considering the highly palindromic character of RUS3A and the perfect conservation of half of the palindromic sequence at an equivalent position of the *D. virilis Rh3* promoter. To test the possibility that a mutant phenotype of RUS3A is masked by functional redundancy of the upstream RUS3B element, the double mutant of RUS3A and RUS3B was constructed and analyzed. Aside from a very modest reduction in head expression levels, four independent transformants of this construct reveal no additional phenotype other than the high body expression found for mutagenesis of RUS3B alone (P[*Rh3.343m1&5CAT*]1–4; Fig. 5A).

Five nonconserved regions of the *D. melanogaster Rh3* promoter in the −124- to −57-bp segment were also individually mutagenized and found to have no role in *Rh3* promoter function. Transformants bearing these mutant constructs display CAT activity profiles indistinguishable from those of nonmutagenized *Rh3–CAT* fusions (P[*Rh3.343m2, m3, m4, m6,* and *m7CAT*]; Fig. 5A). A puzzling result of this analysis is that 5′ deletion of sequences between −137 and −66 bp abolishes *Rh3* promoter activity, yet virtually complete mutagenesis of this region yields no loss-of-expression phenotypes. One possible explanation is that wild-type sequences between −343 and −137 bp in these mutant *Rh3* promoters can substitute for mutagenized *cis*-acting elements in the −137- to −66-bp region.

Oligonucleotide-directed mutagenesis of the *Rh4* promoter fragment extending from −472 to +7 bp reveals that all three highly conserved sequences are necessary for proper R7-specific gene expression. Mutation of the *Rh4*-specific upstream element RUS4A completely eliminates promoter activity in 12 independent transformant lines (P[*Rh4.472m1CAT*]1–12; Fig. 5B). Expression of an *Rh4* promoter bearing a mutagenized RCS I is reduced 5- to 50-fold relative to nonmutagenized *Rh4* promoters and is no longer localized to R7 photoreceptor cells (P[*Rh4.472m2CAT*]1–11; Fig. 5B). In spite of the large quantitative variations among the 11 different lines, individual lines display CAT activity levels in sev^{d2} or $boss^{3991}$ heads virtually identical to those in wild-type heads. Mutation of the *Rh4* RCS II produces a phenotype similar to but less severe than mutation of RCS I (P[*Rh4.472m3CAT*]1–19; Fig. 5B). Expression is reduced 3- to 20-fold relative to nonmutagenized *Rh4–CAT* constructs and R7 cell-type specificity is only par-

Figure 5. Histograms summarizing the mutagenesis data for the *D. melanogaster Rh3* promoter (*A*), the *D. melanogaster Rh4* promoter (*B*), and the RCS I–RCS II region exchanges between the *Rh3* and *Rh4* promoters (*C*). CAT assay data were obtained and plotted as described in the legend to Fig. 3 and in Materials and methods. Mutagenesis was performed on a wild-type *Rh3* promoter fragment extending from −343 to +18 bp (see P[*Rh3.343CAT*]; Fig. 3A) and on a wild-type *Rh4* promoter fragment extending from −472 to +7 bp (see P[*Rh4.472CAT*]; Fig. 3B). The wild-type sequence of the mutagenized region (*wt*) and the sequences of the individual mutagenizing oligonucleotides (*mut*) are aligned beneath (*A* and *B*) or beside (*C*) the histogram. The asterisks (*) in *C* denote the individual nucleotides mutated in each construct. In *A* and *B*, transformant lines corresponding to each mutagenized promoter construct are encompassed by the underlying bracket and are labeled with the construct designation used in the text. Solid lines indicate the mutagenized sequence corresponding to each bracketed set of transformant lines. In *A*, m1&5 refers to an *Rh3* promoter doubly mutagenized with both m1 and m5. CAT activity levels in body tissues of P[*Rh3.343m1CAT*] and P[*Rh3.343m1&5CAT*] are 1.5- to 2.5-fold less in sev^{d2} than in wild type; we have not yet determined whether this effect is due to the sev^{d2} mutation or to genetic modifiers present in the sev^{d2}; ry^{506} parental strain. In *B*, the head CAT activity levels of the P[*Rh4.472m2CAT*] lines in wild-type and sev^{d2} or $boss^{3991}$ genetic backgrounds have been offset to reveal their similarity. As in Fig. 3, shaded bars show CAT activity levels in wild-type tissues, and solid bars show CAT activity levels in sev^{d2} or $boss^{3991}$ tissues; absence of bars means <0.1% CAT activity, and A denotes the average values for all transformant lines of a given construct. All CAT activity levels are normalized to the wild-type head value of the standard reference line P[*Rh3.2600CAT*]1 (Fig. 3A). Evolutionarily conserved sequences are boxed and labeled as in Fig. 4. Arrows denote the direction of transcription.

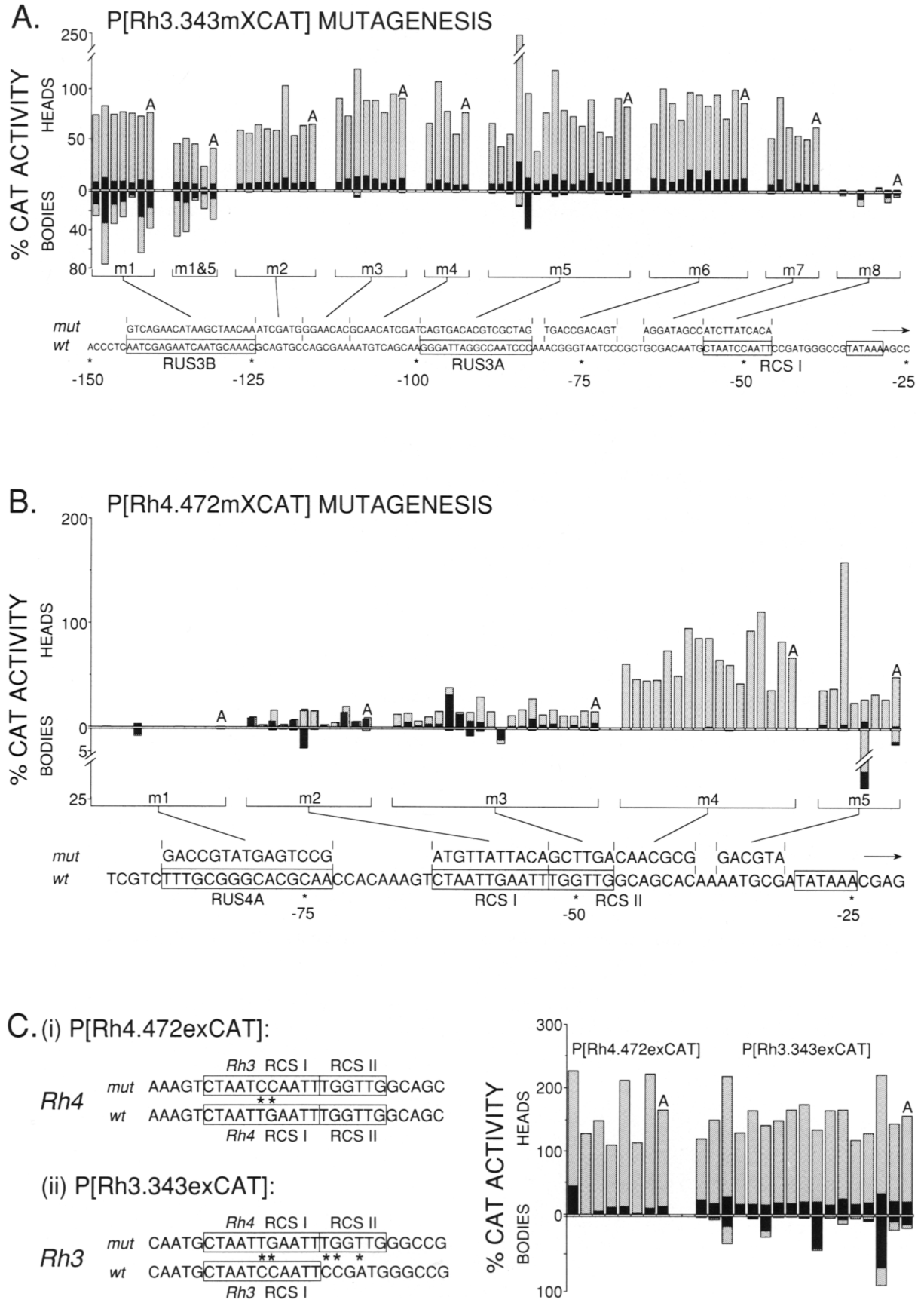

Figure 5. (*See preceding page for legend.*)

tially impaired. As with the *Rh3* promoter mutagenesis, alteration of two different nonconserved sequences within the proximal *Rh4* promoter region does not affect promoter function significantly (P[*Rh4.472m4* and *m5CAT*]; Fig. 5B).

The mutant phenotypes of RCS I and RCS II of the *Rh4* promoter suggest that RCS II may serve as an accessory element for RCS I. Consistent with this proposal, RCS II is located immediately adjacent to one end of RCS I (Fig. 4). Further evidence for an accessory function of RCS II is provided by the analysis of transformants bearing *Rh4*-CAT fusions with mutated RCS I and RCS II sequences in a *glass*^{3} (*gl*^{3}) genetic background, which eliminates all photoreceptor cells (Moses et al. 1989). A total of 39 selected transformant lines bearing rhodopsin promoter–*CAT* fusions have been analyzed in *gl*^{3} flies, representing a diverse collection of *D. melanogaster Rh3* and *Rh4* nonmutagenized promoters of different sizes, *D. virilis Rh3* and *Rh4* promoters, *Rh3* and *Rh4* promoters mutant for each of the conserved sequences, and a single *Rh1* promoter bearing a mutagenized RCS I sequence (from Mismer and Rubin 1989). With the exception of the *Rh4* RCS I and RCS II mutants, CAT activity levels of all these transformants were much lower in *gl*^{3} heads, as compared to *sev*^{d2} or *boss*^{3991} heads (data not shown), consistent with most ectopic non-R7 expression in these lines being localized to other photoreceptor cells. In contrast, all five transformants mutant for *Rh4* RCS I (P[*Rh4.472m2CAT*]1, 7, 8, 10, and 11) and both mutant for *Rh4* RCS II (P[*Rh4.472m3CAT*]5 and 14) displayed 1.5- to 2-fold more expression in *gl*^{3} heads than in wild-type, *sev*^{d2} or *boss*^{3991} heads (data not shown). Although we do not understand the basis of this effect, it suggests a functional relationship between RCS I and RCS II. No CAT activity was detected in *sine oculis* heads of a single tested transformant line of the *Rh4* RCS I mutant construct (P[*Rh4.472m2CAT*]5), indicating that the ectopic non-R7 expression of this fusion gene detected in *sev*^{d2}, *boss*^{3991}, and *gl*^{3} heads is still localized to visual system structures (data not shown). The contiguous arrangement of RCS I and RCS II in the *Rh4* promoter, as well as their similar phenotypic behavior when mutated, suggest that these two *cis*-acting elements comprise a single functional unit. The finding that the *D. virilis Rh4* promoter, in which this unit is inverted, is functionally equivalent to its *D. melanogaster* counterpart demonstrates that the RCS I–RCS II unit is capable of working in an orientation-independent manner.

RCS I and RCS II exchanges and hybrid promoter experiments

Evolutionary considerations and promoter mutagenesis data immediately suggest an attractive model for combinatorial control of transcription in the *Drosophila* rhodopsin genes. All four paired rhodopsin promoters of *D. melanogaster* and *D. virilis* contain an RCS I element, in some cases coupled with RCS II, immediately upstream of the TATA box (Fig. 4). More distal RUS elements, on the other hand, are specific to each pair of corresponding rhodopsin gene promoters from the two species. The mutagenesis results presented here and elsewhere (Mismer and Rubin 1989) have demonstrated the functional importance of all RCS and RUS elements tested, with the exception of RUS3B, in the *D. melanogaster Rh1*, *Rh3*, and *Rh4* promoters. For each rhodopsin gene, the proximal regulatory region containing RCS I (or RCS I–RCS II) and the TATA box may therefore constitute a functionally equivalent promoter core, with cell-type specificity determined by unique upstream sequences. Support for this model is furnished by two additional lines of investigation.

In the first set of experiments, oligonucleotide-directed mutagenesis was used to exchange the RCS I and RCS II sequences of *Rh3* and *Rh4* to test directly their functional equivalency. The *D. melanogaster* and *D. virilis Rh3* RCS I sequence CTAATCCAATT differs from the RCS I sequences of the remaining six rhodopsin promoters, which define the consensus RCS I sequence CTAATTGAATT (Fig. 4). The *D. melanogaster Rh4* RCS I sequence matches this consensus. Seven transformant lines of a 472-bp *Rh4–CAT* construct in which the *Rh4* RCS I has been altered to match the *Rh3* RCS I exhibit normal R7-specific gene expression (P[*Rh4.472ex CAT*] 1–7; Fig. 5C). CAT activity levels in heads of most of these transformants are elevated 1.5- to 2.5-fold relative to levels detected in heads of transformants bearing the nonmutagenized 472-bp *Rh4–CAT* construct. Because conversion of the *Rh4* RCS I to the *Rh3* RCS I entails only a 2-bp substitution (TG to CC), this quantitative effect most likely reflects a slightly higher binding affinity of the *Rh3* RCS I sequence for the putative *trans*-acting factor(s) interacting with this element.

The converse RCS exchange was performed by mutagenizing the RCS I sequence of the 343-bp *Rh3* promoter to match that of *Rh4* (and the consensus) and to replace simultaneously the adjacent 3′ hexanucleotide with an RCS II element. This *Rh3* promoter, now bearing an *Rh4*-like RCS I–RCS II region, was fused to *CAT* and assayed in 16 independent transformant lines (P[*Rh3.343exCAT*]1-16; Fig. 5C). All lines display an expression profile similar to nonmutagenized *Rh3–CAT* transformants. Approximately 90% of head CAT activity is localized to R7 photoreceptor cells, with the remaining 10% presumably attributable to dorsal marginal R8 cell expression. However, the quantitative levels of head CAT activity in these transformants are generally 1.5- to 2.5-fold higher than in transformants bearing the nonmutagenized 343-bp *Rh3–CAT* construct. This increase is most easily interpreted as the net effect of two alterations made to the *Rh3* promoter. Conversion of the *Rh3* RCS I to an *Rh4* RCS I is expected to reduce promoter strength slightly (by analogy to P[*Rh4.472exCAT*]; Fig. 5C), whereas inclusion of RCS II is expected to increase promoter activity moderately (by analogy to P[*Rh4.472m3CAT*]; Fig. 5B). Disregarding minor quantitative effects, these experiments clearly demonstrate that the *Rh3* RCS I and the *Rh4* RCS

I–RCS II unit are functionally interchangeable despite their differing DNA sequences.

As a second test of the bipartite functional organization of the rhodopsin promoters, hybrid promoters consisting of distal (putative cell-type specificity) regions and proximal (putative core) regions of different rhodopsin promoters were constructed, fused to *CAT*, and assayed in transformed flies. The *D. melanogaster Rh2*, *Rh3*, and *Rh4* promoters were chosen for these experiments, as cell-type specificity of the resulting hybrid promoters is easily determined by measuring CAT activity in wild-type transformants, transformants lacking R7 photoreceptors (*sev*^{d2} or *boss*^{3991}), and transformants lacking ocellar photoreceptors (*oc* for autosomal inserts or *noc*^{4} for X-linked inserts). Proximal and distal promoter segments were derived from an *Rh2* promoter extending from −183 to +32 bp, an *Rh3* promoter extending from −137 to +18 bp, and an *Rh4* promoter extending from −159 to +7 bp. Previous analysis has shown that this *Rh2* promoter fragment is active at wild-type levels in ocellar photoreceptors (Mismer et al. 1988). The *Rh3* and *Rh4* promoter fragments selected for these experiments are the smallest ones still capable of generating nearly wild-type levels of R7-specific gene expression. A *Bgl*II restriction site was inserted immediately 5′ to the RCS I element in each of these promoters, such that the last 2 bp of the *Bgl*II site (AGATCT) coincides with the initial CT nucleotides of RCS I, and was used to construct all six possible pairwise hybrid promoter–*CAT* fusions.

hybrid promoter transformant line	% CAT activity: bodies	heads: wild-type	heads: *sev* or *boss*	heads: *oc* or *noc*
P[*Rh2/4CAT*]1	<0.1	10.3	20.5	<0.1
2	<0.1	8.3	11.7	<0.1
3	0.1	130.0	117.0	<0.1
4	<0.1	4.6	13.5	0.4
5	0.3	138.7	150.8	<0.1
6	<0.1	44.6	56.6	<0.1
average	<0.1	56.1	61.7	<0.1
P[*Rh2/3CAT*]1	0.2	1.1	1.1	0.2
2	<0.1	<0.1	<0.1	<0.1
3	<0.1	6.7	5.9	0.2
4	0.3	8.7	4.2	<0.1
5	0.1	9.2	7.5	<0.1
6	0.4	0.5	0.8	<0.1
7	<0.1	1.5	1.8	<0.1
8	<0.1	0.6	0.9	<0.1
9	<0.1	1.5	1.4	0.2
average	0.1	3.3	2.6	<0.1
P[*Rh3/4CAT*]1	<0.1	53.7	0.6	30.0
2	0.8	25.2	<0.1	13.5
average	0.4	39.5	0.3	21.8
P[*Rh3/2CAT*]1	<0.1	0.5	<0.1	<0.1
2	0.2	1.5	<0.1	0.7
3	<0.1	6.2	<0.1	1.7
4	<0.1	6.1	0.4	1.9
5	0.3	0.8	<0.1	1.4
6	<0.1	3.8	0.6	4.5
average	<0.1	3.2	0.2	1.7
P[*Rh4/3CAT*]1-7	<0.1	<0.1	<0.1	<0.1
P[*Rh4/2CAT*]1-13	<0.1	<0.1	<0.1	<0.1
reference lines:				
P[*ry; Rh2(-4300/+32)-CAT*]2		100		
P[*Rh3.2600CAT*]1		970		

The expression patterns of four of these hybrid promoter constructs in different genetic backgrounds are consistent with the model presented above. Hybrid promoters in which the distal promoter segment of *Rh2* is fused to the proximal promoter regions of either *Rh3* or *Rh4* are active exclusively in ocellar photoreceptor cells (P[*Rh2/3CAT*]1–9 and P[*Rh2/4CAT*]1–6; Fig. 6). In contrast, hybrid promoters combining the *Rh3* distal promoter region with proximal promoter segments of either *Rh2* or *Rh4* display R7-specific expression patterns (P[*Rh3/2CAT*]1–6 and P[*Rh3/4CAT*]1–2; Fig. 6). The activities of these hybrid promoter–*CAT* constructs are difficult to quantitate accurately, as they are expressed at very low levels relative to their parental *Rh2*, *Rh3*, and *Rh4* promoters (precluding a *lacZ* analysis). Nevertheless, the transformant lines exhibiting higher levels of expression demonstrate convincingly that cell-type specificity is dictated by the distal promoter component for each of these four hybrid promoters. The remaining two hybrid promoters, in which the distal promoter segment of *Rh4* is matched with the proximal promoter re-

Figure 6. Expression patterns of hybrid rhodopsin promoter–*CAT* fusion genes. The left-most column lists all independent transformant lines obtained for the six hybrid promoter–*CAT* fusion constructs. Each construct is named according to the sources of the distal and proximal promoter segments joined at RCS I. For example, P[*Rh2/4CAT*] contains a distal *Rh2* promoter fragment joined to a proximal *Rh4* promoter fragment. The exact composition of each hybrid promoter may be found in the text and in Materials and methods. The four numerical columns show transformant line CAT activity levels in wild-type bodies, wild-type heads, heads lacking R7 cells (*sev*^{d2} or *boss*^{3991}), and heads lacking ocelli (*oc* or *noc*^{4}). Shaded columns reveal the genotypes in which CAT activity is eliminated, allowing the expression of four hybrid promoter constructs to be localized to either R7 cells or the ocelli. Because of the quantitatively low levels of expression of these hybrid promoter–*CAT* fusions, duplicate CAT assays were performed for 5 hr instead of 2 hr and CAT activity is expressed relative to wild-type head levels of a 4.3-kb *Rh2* promoter–*CAT* fusion (P[*ry; Rh2(−4300/+32)–CAT*]2; Mismer et. al. 1988). For comparison, the wild-type head CAT activity of P[*Rh3.2600CAT*]1, the standard reference line of Figs. 3 and 5, was extrapolated from head extract dilutions included in these assays and is also shown. Error is estimated to be not greater than 30%; <0.1 means that CAT activity was not detected above background level.

gions of either *Rh2* or *Rh3*, are completely nonfunctional in this assay (P[*Rh4/2CAT*]1–13 and P[*Rh4/3CAT*]1–7; Fig. 6). Proper function of the *Rh4* distal promoter region may thus depend on sequences specific to the *Rh4* proximal promoter segment, such as RCS II, or on particular spatial requirements among different *cis*-acting elements not preserved in these two hybrid promoter constructs.

Discussion

Combinatorial control of Drosophila *rhodopsin gene regulation*

The major result of this study is that the four rhodopsin promoters all share a simple bipartite structure. The 60- to 70-bp region immediately upstream of the transcriptional start site apparently constitutes a functionally equivalent proximal promoter core for each rhodopsin gene. Determinants of cell-type specificity generally reside within a 100- to 200-bp segment of each promoter immediately distal to the core region. The best evidence for this model is provided by the expression patterns of hybrid promoter constructs that mismatch proximal and distal promoter regions of the *Rh2*, *Rh3*, and *Rh4* genes. Cell-type-specific expression of four such hybrid promoter constructs in either R7 or ocellar photoreceptors is dictated by the distal promoter segment in each case.

A striking feature of all four *D. melanogaster* rhodopsin promoters is that *cis*-acting DNA sequences sufficient for highly cell-type-specific gene expression reside within very small (<300 bp) upstream regulatory regions (*Rh1*, Mismer and Rubin 1987; *Rh2*, Mismer et al. 1988; *Rh3* and *Rh4*, this report). *D. virilis Rh3* and *Rh4* promoter fragments of comparable sizes also function in the appropriate R7-specific manner when introduced into *D. melanogaster*. The small sizes of the rhodopsin gene promoters are in marked contrast to those of many developmentally regulated *Drosophila* genes (see, e.g., Hiromi et al. 1985) and may reflect their relatively simple expression patterns in single differentiated cell types. In practical terms, the small sizes of these promoters have greatly facilitated further characterization of their *cis*-acting requirements by oligonucleotide-directed mutagenesis of evolutionarily conserved sequences.

Between this report and a previous study (Mismer and Rubin 1989), a total of 31 sequences of the *Rh1*, *Rh3*, and *Rh4* promoters have been separately mutagenized and functionally assayed in vivo. Mutagenesis seriously impairs promoter function for 7 of the 8 sequences conserved between *D. melanogaster* and *D. virilis*, whereas mutagenesis does not alter normal expression patterns for the 23 nonconserved regions. Moreover, the one conserved sequence that fails to reveal a mutant phenotype in our assay (RUS3A) is specifically protected from DNase I digestion by a factor present in *Drosophila* adult head nuclear extracts (E. O'Neill, G.M. Rubin, and R. Tjian, unpubl.). However, a limitation of this approach is revealed by the *D. melanogaster Rh4* promoter deletion analysis. This analysis has localized essential regulatory sequences between −159 and −123 bp, a region containing no obvious homologies to the *D. virilis Rh4* promoter. Nevertheless, our data indicate that evolutionary considerations are a useful guide for designing deletion and mutagenesis studies of gene regulatory regions.

The dominant feature of each rhodopsin proximal promoter region, aside from the TATA box, is the presence of a motif (RCS I) corresponding to the consensus sequence CTAATTGAATT. For *Rh1*, mutagenesis of RCS I leads to a pronounced reduction in promoter strength with no loss of cell-type specificity (Mismer and Rubin 1989). Mutation of the *Rh3* RCS I essentially eliminates promoter function, and mutation of the *Rh4* RCS I results in low levels of ectopic expression in adult visual system structures. The mutant phenotype of the *Rh2* RCS I has not yet been examined.

Whereas RCS I and other proximal core sequences do not determine photoreceptor subclass specificity, they may nevertheless serve as less restrictive tissue-specificity determinants. Sequence motifs closely matching the RCS I consensus have been noted (Mismer and Rubin 1989; M. Fortini and C.S. Zuker, unpubl.) in the proximal 5′ regions of several *Drosophila* genes expressed specifically in all or part of the photoreceptor cell population, namely *trp* (Montell and Rubin 1989; Wong et al. 1989), *ninaA* (Schneuwly et al. 1989; Shieh et al. 1989), *ninaC* (Montell and Rubin 1988), *chp* (Reinke et al. 1988), and *arrestin* (Smith et al. 1990). RCS I may thus confer on a promoter the ability to be potentially activated in all photoreceptor cells, with more restricted cell-type specificities determined by upstream *cis*-acting elements.

The exact roles played by these distal promoter RUS elements in restricting rhodopsin gene expression to individual photoreceptor cell types are not well understood. Three different mutations affecting RUS1A have been found previously to cause ectopic expression of *Rh1–CAT* constructs in body tissues without perturbing the specificity of *Rh1–lacZ* expression in R1–R6 photoreceptor cells (Mismer and Rubin 1989). The fact that the *ninaA* gene—which, within the retina, is also expressed only in R1–R6 photoreceptors—contains two RUS1A-like sequences and one RCS I-like motif within the region immediately upstream of the TATA box (M.E. Fortini and C.S. Zuker, unpubl.) suggests that RUS1A may nevertheless contribute to the restricted expression of *Rh1* in outer photoreceptors only. The *Rh3*-specific element RUS3B, like RUS1A, displays a mutant phenotype of elevated body expression. On the other hand, partial deletion of RUS3B in P[*Rh3.137CAT*] reveals a preferential loss of dorsal marginal R8 expression with no increase in body expression. Whether RUS1A and RUS3B serve to repress the *Rh1* and *Rh3* genes in body tissues and whether they participate in the regulation of these genes in photoreceptor cells of the eye are still unresolved issues. Mutagenesis of RUS4A yields a complete loss-of-expression phenotype, demonstrating only that this element is somehow required for *Rh4* promoter function.

The hybrid promoter experiments avoid these ambiguities by demonstrating in a positive assay those cell-type-specific regulatory features of distal promoter sequences that can be conferred on a heterologous proximal promoter core. The results of these experiments provide a glimpse into the underlying logic of combinatorial control in the transcriptional regulation of a small set of eukaryotic genes. In every photoreceptor cell, common transcription factors might be expected to interact with rhodopsin gene proximal promoter sequences such as RCS I and RCS II. All of the rhodopsin genes in the cell would then be poised for activation, but only one would be activated via specific interactions of its distal promoter sequences (such as RUS elements) with a particular constellation of *trans*-acting factors characteristic of that photoreceptor cell type. Interactions of factors bound upstream with components of the transcriptional apparatus, such as TATA factors and RNA polymerase II, may be mediated through the factor(s) associated with RCS I or RCS I–RCS II. Distal *Rh3* and *Rh4* promoter sequences are unable to direct a coherent expression pattern of any sort when RCS I has been removed by mutagenesis. Furthermore, upstream enhancer regions of *Rh1* are nonfunctional when fused to a heterologous *hsp70* promoter TATA box region (Mismer and Rubin 1989). Precedents for a similar mediation of the regulatory effects of factors bound distally via those bound more proximally have been noted in the mammalian SV40 promoter (Courey et al. 1989), the SV40 enhancer–β-globin promoter interaction (Treisman and Maniatis 1985), the *Drosophila Ubx* promoter (Biggin et al. 1988; Müller et al. 1989), the *Drosophila Ddc* promoter (Bray et al. 1988), and the *Drosophila Adh* promoter (Fischer and Maniatis 1988).

Efforts to isolate the *trans*-acting factors that regulate expression of the *Drosophila* rhodopsin genes are currently under way. Comparisons of their distribution patterns within the adult photoreceptor cells and throughout the organism as a whole should allow a critical evaluation of this model of combinatorial control in rhodopsin gene regulation. If the model is correct, there is no reason to suspect that these factors will not be present in a variety of different tissues and cell types. The essential constraint is that a full complement of *trans*-acting factors capable of activating one of the rhodopsin promoters must be found only in the appropriate photoreceptor cell type. Within the photoreceptor cell population, the factor(s) interacting with RCS I and perhaps RCS II are expected to be present in all cell types. At least some of the factors interacting with the distal RUS regions of the rhodopsin promoters should exhibit more restricted distributions within these cells, although not necessarily to single photoreceptor cell types.

Regulation of R7 opsin expression patterns

The expression patterns of *Rh3–lacZ* and *Rh4–lacZ* fusion genes presented here provide further insight into the organization of the *Drosophila* visual system. The relative abundance of *Rh3*-expressing (30%) and *Rh4*-expressing (70%) R7 photoreceptors across most of the retina, as well as expression of *Rh3* in dorsal marginal R7 and R8 cells, allows the *Rh3* and *Rh4* opsins to be assigned as the respective *Drosophila* homologs of the *Musca* and *Calliphora* 7p and 7y opsins (Kirschfeld et al. 1978). In vivo epifluoresence studies have shown that R7 photoreceptors of the 7p and 7y classes are distributed in an apparently random fashion across most of the compound eye in *M. domestica* (Franceschini et al. 1981; Hardie et al. 1981; Hardie 1985). The distribution pattern displays no dorsoventral or bilateral symmetries within a single eye, and no reproducible patterns are noticed among different eyes, even between the two eyes of the same individual. Spectral sensitivity measurements in the larger dipterans unequivocably demonstrate the presence of two distinct R8 visual pigments, termed the 8p and 8y opsins, each expressed specifically in R8 cells corresponding to a particular subclass of overlying R7 cells (Smola and Meffert 1979; see also Hardie 1985, 1986). The central photoreceptor cell populations of *Musca* and *Calliphora* thus comprise a random distribution of matched 7p/8p and 7y/8y pairs. The *cis*-acting regulatory regions of these four opsin genes must be capable of directing highly specific expression of the R7 and R8 opsin genes in strictly nonoverlapping subpopulations of their respective photoreceptor cell types while ensuring that the two resulting stochastic patterns coincide completely with each other. Isolation of the corresponding R8 opsin genes of *D. melanogaster* and comparison of their regulatory regions with the *Rh3* and *Rh4* promoters may provide some insight into this remarkable expression pattern.

Models may be devised envisioning the stochastic pattern of R7 opsin gene expression as the consequence of rather direct regulatory interactions between their promoters in terminally differentiated R7 photoreceptor cells. For example, competition between the *Rh3* and *Rh4* promoters for a limited supply of common *trans*-acting factors or antagonistic effects among different factors that activate one promoter while repressing the other could, in principle, generate the observed mutually exclusive distributions of *Rh3*- and *Rh4*-expressing R7 subclasses. However, the coordinate expression of R7 and R8 opsin genes assumed for *Drosophila* by analogy to other dipterans makes such scenarios unlikely. The compound eye photoreceptors are recruited from a homogeneous population of pluripotent precursor cells of the late third-instar larval eye disc and are not related by lineage (see Tomlinson 1988; Ready 1989; Rubin 1989; Zipursky 1989). For this reason, we favor a model in which early regulatory events of a stochastic nature establish the subclass identity of one of the undifferentiated central photoreceptor cells, which, in turn, communicates this decision to the other member of the pair in the developing ommatidial cluster. For example, local fluctuations in inductive signals across the eye disc may partition the R8 cells, the first ommatidial cells to undergo cell fate specification, into two differentiation

subclasses having a ratio of ~70 : 30. Next, the *sev*- and *boss*-mediated signaling event by which the R8 cell induces R7 cell formation might be modulated differently for each R8 subclass, causing R7 precursors to correctly adopt either the *Rh3*- or the *Rh4*-expressing differentiation pathway. Thus, within the regulatory hierarchies controlling development of these cell types, the processes that ultimately generate the stochastic expression patterns of the *Drosophila* R7 (and presumably R8) opsin genes may operate considerably upstream of the rhodopsin promoters. Consistent with this idea, the *Drosophila* R7 opsin gene promoters seem as different from each other in terms of functional organization as they are from the promoters of the R1–R6 and ocellar rhodopsin genes (Fig. 4). Moreover, detailed characterizations of *Musca* and *Calliphora* central photoreceptor cells suggest that the two subclasses of both R7 and R8 cells display subtle differences in numerous anatomical and physiological features, including rhabdomere length and twist, the fine structure of the transition point between R7 and R8 rhabdomeres, nuclear location, and the presence of photosensitizing and screening accessory pigments (Kirschfeld et al. 1977, 1978; Wunderer and Smola 1982a; Hardie 1985). In light of these considerations, the assignment of R7 (and R8) subclasses as members of single photoreceptor cell types may be somewhat artificial.

Functional properties of Drosophila *R7 opsins*

The rich variety of spectral types that distinguish the dipteran central photoreceptors from the spectrally uniform outer photoreceptors has led numerous investigators to speculate that they may be involved in color vision, similar to the cones of the vertebrate retina (Menne and Spatz 1977; Franceschini 1984; Hardie 1985, 1986). Defective color-specific phototactic responses are, in fact, observed for the *Drosophila sev* mutant (Schümperli 1973; Harris et al. 1976; Heisenberg and Buchner 1977; Fischbach 1979). The idea that the two R7 cell subclasses may comprise part of a dipteran color vision system would gain credence if it could be demonstrated that their inputs are processed independently by the brain. Interestingly, Golgi impregnations of *Drosophila* photoreceptor neurons have revealed long and short synaptic terminal variants in both the R7 and R8 target layers of the medulla (Fischbach and Dittrich 1989). The long variants were found to occur more rarely; however, this technique did not allow the two variants to be correlated with specific *Rh3*- or *Rh4*-expressing R7 cells. The use of rhodopsin promoter-driven histological marker genes capable of differentially labeling the axonal projections of each R7 subclass holds much promise for this line of investigation.

Expression of *Rh3–lacZ* constructs in a small group of ~25 dorsal marginal R7 and R8 photoreceptor pairs constitutes a striking deviation from the stochastic R7-specific expression of *Rh3* across the remainder of the *Drosophila* compound eye. An analogous region of R7 and R8 cells (termed 7marg/8marg), both containing the 7p opsin, have been described in *Musca* and *Calliphora* (Hardie 1985, 1986). The labeling of these cells with Lucifer yellow (Hardie 1984) and cobalt (Strausfeld and Wunderer 1985) has revealed that they project long axons with enlarged terminals to the dorsal posterior medulla, consistent with the β-galactosidase staining patterns of the *Rh3–lacZ* transformant lines described in this paper. A more detailed description of the *Rh3–lacZ* staining pattern in the medulla neuropil subserving these specialized central photoreceptor cells of *D. melanogaster* will be presented elsewhere (M.E. Fortini and G.M. Rubin, in prep.).

Specialized dorsal marginal ommatidia with greatly enlarged central rhabdomeres have been identified in a number of dipteran species, including *Drosophila* (Wada 1971, 1974). Detailed characterization of these photoreceptors in *Musca* and *Calliphora* has shown that the paired R7 and R8 cells are extremely sensitive to different e-vector directions of polarized light (Wunderer and Smola 1982b; Hardie 1984). Similar polarized light-sensitive photoreceptors have also been found in the dorsal marginal eye regions of bees and desert ants. Selective masking experiments have shown that in these insects, the dorsal marginal ommatidia are used to navigate by the ultraviolet polarized light patterns of the sky (Labhart 1980; Wehner 1982, 1989). *D. melanogaster* is also apparently capable of orienting with respect to the e-vector direction of polarized light (Stephens et al. 1953; Wolf et al. 1980). Navigation not only requires that the polarized light composition of the sky be measured with respect to two different planes but also that absorbance differences due to changes in e-vector direction be distinguished from those due to changes in intensity or wavelength of the light (Autrum and Stumpf 1950; Wehner 1982, 1989; Hardie 1984). If both central photoreceptors contain the same rhodopsin, the latter absorbance differences are automatically normalized such that any net absorbance difference between the two paired cells can only be due to polarization of light in the dorsal contralateral visual field. These constraints provide a clear rationale for expression of *Rh3* in paired R7 and R8 photoreceptors at the dorsal eye margin in *Drosophila*.

Concluding remarks

Recent genetic and molecular studies have implicated *sev*, *boss*, and other loci in the early events of ommatidial assembly in *D. melanogaster* (for review, see Tomlinson 1988; Ready 1989; Rubin 1989; Zipursky 1989). The analysis of the regulatory regions of rhodopsin genes expressed in specific subsets of adult photoreceptor cells offers a complementary approach toward investigating ommatidial development. The expression patterns of these genes must reflect, to a large extent, unique gene regulatory properties of the ommatidial photoreceptor cells established during their earlier determination and differentiation. Identification of transcription factors that interact with the rhodopsin promoters may thus help narrow the gap in our understanding of how genes

such as *sev* and *boss* exert their regulatory effects via sets of downstream genes. Through this approach we hope ultimately to reconstruct the hierarchy of molecular events, whereby positional cues and cell–cell communication in the developing eye disc eventually give rise to the precise array of terminally differentiated cell types of the adult compound eye.

Materials and methods

DNA manipulations

DNA manipulations, including restriction endonuclease digestions, ligations, nick-translations, bacterial transformations, and plasmid DNA isolations, were performed according to standard procedures (Maniatis et al. 1982).

Isolation of D. virilis *rhodopsin genes*

The *D. virilis* rhodopsin genes were isolated from a *D. virilis* genomic DNA library prepared in λ EMBL-3 (gift of Dr. M. Scott, University of Colorado, Boulder) by screening with nick-translated *D. melanogaster* probes under the following conditions: 2× SSC, 20% formamide, 0.2% SDS, 5× Denhardt's solution [0.1% Ficoll, 0.1% polyvinylpyrrolidone (PVP), 0.1% bovine serum albumin (BSA)], 100 μg/ml herring sperm DNA at 45°C, followed by three 1-hr washes in 2× SSC, and 0.2% SDS at 45°C. A precise description of the *D. melanogaster* rhodopsin gene probes used will be available elsewhere (Fortini 1990). A limited amount of protein-coding region sequence was obtained for the *D. virilis* opsin genes to allow each one to be correctly identified as the homolog of a particular *D. melanogaster* opsin gene.

DNA sequence analysis

DNA sequencing was performed according to the dideoxy chain-termination method (Sanger et al. 1977). Promoter sequences obtained during this study (see legend to Fig. 4) were determined on both DNA strands. Pairwise homology searches were performed in all combinations among the eight available *D. melanogaster* and *D. virilis* rhodopsin promoters on a SUN computer, using IntelliGenetics sequence analysis software.

Construction of rhodopsin promoter fusion genes

All 45 rhodopsin promoter fusions described in this paper were made by a simple three-step cloning procedure. First, appropriate DNA manipulations were performed to generate the desired promoter fragments. Second, the promoter fragments were fused to *CAT* or *lacZ* in the vector pHSS7 (Seifert et al. 1986). For all promoter fusions to *CAT*, we used the pDM47 vector (Mismer et al. 1988), a pHSS7 derivative bearing a *CAT* transcriptional fusion module. The polylinker of pHSS7 is bordered by *Not*I sites, which are not found in any of the rhodopsin promoter or reporter gene sequences used here. Third, the resultant promoter fusions were removed from pHSS7 as intact *Not*I fragments and subcloned into the unique *Not*I site of the modified Carnegie 20 vector pDM30 (Mismer and Rubin 1987).

Cloning steps were designed to minimize nonessential differences among the various DNA constructs. All promoter fusions described here were inserted into pDM30 in the same orientation [head to head with respect to the *rosy*$^+$ (*ry*$^+$) selectable marker gene of pDM30]. All promoter–*CAT* fusions also utilize the same *Kpn*I site of pDM47 as the sequence junction. The three rhodopsin promoter–*lacZ* fusions are also equivalent to one another in terms of sequences present at the junction. Moreover, all constructs using a given promoter (e.g., *D. melanogaster Rh3*, *D. virilis Rh4*) are identical with respect to 5′-untranslated leader sequences and polylinker sequences present at the promoter–reporter gene junction (see below for details).

Rh3–lacZ *and* Rh4–lacZ *fusions*

For *Rh3*, a genomic *Hin*dIII–*Msp*I promoter fragment extending from −2.6 kb to +18 bp of the 22-bp *Rh3* untranslated leader sequence was subcloned into *Hin*dIII/*Acc*I-cleaved pIC-20R (Marsh et al. 1984). The entire insert was then removed as a *Bgl*II–*Eco*RI fragment and transferred into *Bam*HI/*Eco*RI-cleaved pHSS7. A *lacZ* transcriptional fusion module was removed as a 4.0-kb *Eco*RI fragment from pDM79 (Mismer and Rubin 1987) and inserted into the *Eco*RI site of this pHSS7 construct. The resulting *Rh3* (−2.6 kb to +18 bp)–*lacZ* fusion was transferred into pDM30 as an intact *Not*I fragment to create pP[*Rh3.2600lacZ*].

A smaller *Rh3* promoter *Hin*dIII–*Kpn*I fragment extending from −343 to +18 bp was used to replace the *Rh1* promoter *Hin*dIII–*Kpn*I fragment of an *Rh1–lacZ* fusion in pHSS7 (Mismer and Rubin 1989). The *lacZ* module in this construct is identical to that in pP[*Rh3.2600lacZ*]. The resulting *Rh3–lacZ* fusion was subcloned into pDM30 as a *Not*I insert to make pP[*Rh3.343lacZ*].

For *Rh4*, a 3.5-kb genomic fragment containing 1.9 kb of upstream *Rh4* sequences in pUC19 was digested with *Xmn*I, which produced a blunt-ended cleavage precisely at the transcriptional start site. A synthetic linker composed of the sequence AGTTCAGGTACCTGCAG was inserted into this cleavage site to reconstitute the first 7 bp of the 87-bp *Rh4* untranslated leader sequence, followed by unique *Kpn*I and *Pst*I restriction sites. The resultant *Rh4* promoter *Bgl*II–*Kpn*I fragment extending from −1.9 kb to +7 bp was used to replace the *Rh1* promoter *Bam*HI–*Kpn*I fragment of the *Rh1–lacZ* fusion in pHSS7 (see above; Mismer and Rubin 1989). The ensuing *Rh4–lacZ* fusion was transferred into pDM30 as a *Not*I fragment to make pP[*Rh4.1900lacZ*].

D. melanogaster Rh3 *and* Rh4 *promoter deletion series*

pP[*Rh3.2600CAT*] was constructed by subcloning an *Rh3* promoter *Xho*I–*Kpn*I fragment extending from −2.6 kb to +18 bp into the *CAT* fusion vector pDM47 and then transferring the resultant fusion into pDM30 as a *Not*I fragment. pP[*Rh3.945CAT*], pP[*Rh3.583CAT*], pP[*Rh3.343CAT*], pP[*Rh3.247CAT*], pP[*Rh3.137CAT*], and pP[*Rh3.66CAT*] were constructed in an analogous fashion by utilizing restriction endonuclease sites that occur naturally within the *Rh3* upstream DNA sequences. pP[*Rh3.99CAT*] was similarly derived from a precursor of pP[*Rh3.343m4CAT*] in which oligonucleotide-directed mutagenesis was used to introduce a *Cla*I site at position −104 bp of the *Rh3* promoter (described below; Fig. 5A).

pP[*Rh4.1900CAT*] was made by inserting an *Rh4* promoter *Cla*I–*Kpn*I fragment extending from −1.9 kb to +7 bp into pDM47 and subcloning the resultant *Rh4–CAT* fusion into pDM30 as a *Not*I fragment. pP[*Rh4.472CAT*] was constructed in an analogous manner by utilizing an *Eco*RI site at −472 bp of the *Rh4* promoter. Exonuclease III digestion (Rogers and Weiss 1980) of the *Rh4* promoter from this *Eco*RI site yielded 5′-deletion end points used to make pP[*Rh4.373CAT*], pP[*Rh4.276CAT*], and pP[*Rh4.159CAT*] by the same cloning protocol. Oligonucleotide-directed mutagenesis of a 472-bp *Rh4* promoter fragment in Bluescript(+) (Stratagene) (described in detail below) was used to generate three further deletions as

follows. pP[*Rh4.123CAT*] and pP[*Rh4.87CAT*] were derived from mutagenesis products in which synthetic *Cla*I sites were introduced at −125 and −92 bp of the *Rh4* promoter. pP[*Rh4.63CAT*] was made from a mutagenized 472-bp *Rh4* promoter bearing a synthetic *Bgl*II site at −67 bp, originally designed to facilitate the construction of hybrid rhodopsin promoters (see below).

For all *Rh3* and *Rh4* promoter fragments <500 bp in size, the precise 5′-deletion end points were determined by DNA sequencing. In some cases, vector polylinker sequences at the deletion end point fortuitously replace several nucleotides deleted from the *Rh3* or *Rh4* promoter. For all constructs, 5′-deletion end point numbers reported here reflect the number of base pairs identical to those of the native rhodopsin promoter sequences. The 3′ ends of all *D. melanogaster Rh3* promoter fragments are identical, consisting of 18 bp of untranslated leader sequence followed by 23 bp of pIC-20R polylinker sequences (from the *Acc*I site to the *Kpn*I site). The 3′ ends of all *D. melanogaster Rh4* promoter fragments are also identical, consisting of 7 bp of untranslated leader sequence terminating in a *Kpn*I site.

D. virilis Rh3–CAT *and* Rh4-CAT *fusions*

A 517-bp *Xba*I–*Sau*3AI fragment of the *D. virilis Rh3* promoter was subcloned into *Xba*I/*Bam*HI-cleaved Bluescript(+), and the amount of 3′ polylinker sequences was reduced by *Sma*I/*Hin*cII digestion followed by religation. This *Sau*3AI site of *D. virilis Rh3* occurs 42 bp downstream of the TATA box and 26 bp upstream of the putative translation initiator ATG codon. The ~500-bp *D. virilis Rh3* promoter module was inserted into pDM47 as an *Xba*I–*Kpn*I fragment, and the resulting fusion was subcloned into pDM30 as a *Not*I fragment to create pP[*Rh3v.500CAT*]. pP[*Rh3v.180CAT*] was similarly derived from the same pDM47 subclone after first removing the *D. virilis Rh3* sequences between the *Xba*I site and a *Cla*I site located 142 bp upstream of the TATA box.

Oligonucleotide-directed mutagenesis was used to insert a unique *Kpn*I site into the *D. virilis Rh4* promoter region at a position 47 bp downstream of the TATA box and 10 bp upstream of the putative translation initiator ATG codon. A 310-bp *Eco*RI–*Kpn*I fragment and a 202-bp *Xba*I–*Kpn*I fragment of this construct were each fused to *CAT* in pDM47, and the resulting fusions were inserted into pDM30 to produce pP[*Rh4v.300CAT*] and pP[*Rh4v.190CAT*].

D. melanogaster Rh3 *and* Rh4 *promoter oligonucleotide-directed mutagenesis*

Oligonucleotide-directed mutagenesis was performed essentially as described in Laski et al. (1986). For the *Rh3* and *Rh4* promoter mutagenesis summarized in Figure 5, the two *Not*I fragments containing the promoter–*CAT* fusions of pP[*Rh3.343CAT*] and pP[*Rh4.472CAT*] (described above) were transferred into Bluescript(+) in the desired orientation. The *Rh3–CAT* single-stranded template was mutagenized separately with nine different oligonucleotides, each consisting of the mutagenizing sequence flanked on either side by 10 bp of the appropriate wild-type sequences [m1–8, Fig. 5A,C(ii)]. The *Rh4–CAT* template was also mutagenized separately with six different oligonucleotides [m1-5, Fig. 5B,C(i)].

Mutagenized promoter fragments were identified by differential hybridization to the corresponding oligonucleotide probe and verified by DNA sequencing. Because the *CAT* module of the single-stranded templates was found to undergo rearrangements occasionally during the mutagenesis procedure, properly mutagenized *Rh3* and *Rh4 Cla*I–*Kpn*I promoter fragments were re-fused to *CAT* in pDM47. These mutagenized promoter–*CAT* fusions were transferred as *Not*I fragments into pDM30 to generate the pP[*Rh3.343m1–8CAT*] series, the pP[*Rh4.472m1–5CAT*] series, pP[*Rh3.343exCAT*] and pP[*Rh4.472exCAT*]. pP[*Rh3.343m1&5CAT*] was constructed by the identical procedure after single-stranded DNA of the oligonucleotide m5-mutagenized *Rh3–CAT* fusion was subjected to a second round of mutagenesis with oligonucleotide m1 (Fig. 5A).

*Hybrid promoter–*CAT *fusion series*

Small *Cla*I–*Kpn*I fragments consisting of the *Rh2* promoter, extending from −183 to +32 bp (Mismer et al. 1988), the *Rh3* promoter, extending from −137 to +18 bp, and the *Rh4* promoter, extending from −159 to +7 bp, were subcloned into Bluescript(+) and used to prepare single-stranded DNA templates. Oligonucleotide-directed mutagenesis was used to introduce a unique *Bgl*II site immediately upstream of RCS I in each promoter, as described above, except that the mutagenizing oligonucleotide for *Rh3* contained 20 bp of 5′-flanking wild-type sequences. Correctly mutagenized promoter sequences were identified by testing for the presence of the *Bgl*II site and verified by DNA sequencing.

All six hybrid promoters were constructed by three-way ligations of the *Cla*I–*Bgl*II distal segment of one promoter and the *Bgl*II–*Kpn*I proximal segment of another promoter into *Cla*I–*Kpn*I-cleaved pDM47. The resultant hybrid promoter–*CAT* fusions were transferred as *Not*I inserts into pDM30 to create pP[*Rh2/3CAT*], pP[*Rh3/2CAT*], pP[*Rh2/4CAT*], pP[*Rh4/2CAT*], pP[*Rh3/4CAT*], and pP[*Rh4/3CAT*].

P-element-mediated germ line transformation

Transformation of *D. melanogaster* was performed as described in Spradling and Rubin (1982) and Rubin and Spradling (1982). Prior to injection, the purified DNAs of all constructs derived from oligonucleotide-directed mutagenesis were confirmed by resequencing the appropriate promoter fragment.

Histochemical stainings

Staining for β-galactosidase activity was performed as described by Mismer and Rubin (1987). For β-galactosidase/Hoechst double staining, sections were not dehydrated after X-gal staining but were immersed in PBS containing 1.0 μg/ml Hoechst 33258 for 2–3 min, washed twice in PBS, and mounted in 70% glycerol in PBS.

CAT enzyme activity assays

To obtain accurate quantitation, CAT activity assays were performed simultaneously on a series of ~30 transformant lines each. For each transformant line, duplicate CAT assays were performed on five heads and five bodies of the appropriate genetic background according to published protocols (Gorman et al. 1982; Mismer and Rubin 1987). Each series included 12–16 wild-type head samples of the standard reference line P[*Rh3.2600CAT*]1 as well as 6–8 nontransformed ry^{506} negative control samples. For all series, excluding the hybrid promoter construct series, CAT assay reactions were performed for 2 hr at 37°C, during which time the reactions were in the linear range. Hybrid promoter CAT assays were allowed to proceed for 5 hr at 37°C due to their low levels of expression.

For autosomal inserts, male transformants were assayed, whereas for X-linked inserts, female transformants were as-

sayed to avoid dosage compensation effects (Spradling and Rubin 1983; Hazelrigg et al. 1984). Standard genetic crosses were employed to produce transformant flies of the appropriate mutant genotypes using the following stocks: sev^{d2}; ry^{506} (sev^{d2}: Banerjee et al. 1987), $boss^{3991}$ ry^{506} ($boss^{3991}$: Reinke and Zipursky 1988), gl^{3} ry^{506} (gl^{3}: Moses et al. 1989), *so*; *TM3*ry^{506}/+ (*so*: Lindsley and Grell 1968), *cm* ct^{6} *oc ptg/CIB*; ry^{506} (*oc*: Lindsley and Grell 1968) and *In(2LR)noc*^{4} *b cn sp/CyO*; ry^{506} (noc^{4}: Ashburner et al. 1983).

CAT assay reaction products were separated by thin-layer chromatography (Gorman et al. 1982) and quantitated by liquid scintillation counting. Counts per minute (CPM) data were used to calculate the CAT activity present in each transformant sample relative to the average P[*Rh3.2600CAT*]1 wild-type head reference value (normalized to 100%) of that series after subtraction of background CPM levels obtained from the nontransformed ry^{506} samples (<1%). For the hybrid promoter transformants, CAT activity is expressed relative to the level present in P[*ry*; *Rh2(−4300/+32)–CAT*]2 reference heads (normalized to 100%). The CAT activity histograms of Figures 3 and 5 were plotted directly from the normalized scintillation counting data using Cricket Graph software.

Acknowledgments

We thank D. Mismer for providing plasmids and fly strains, C. Zuker for providing *Rh3* genomic subclones, and C. Montell for providing *Rh4* genomic subclones. We gratefully acknowledge M. Scott for generously providing us with his *D. virilis* genomic library, S.L. Zipursky for making $boss^{3991}$ flies available prior to publication, M. Fuchs and D. Schneider for obtaining the *D. virilis Rh1* promoter sequence, and D. Lin and M. Rexach for assisting with the *D. virilis Rh2* cloning. A special debt of gratitude is owed to J. Hirsh for initially suggesting the isolation of the *D. virilis* rhodopsin genes. We thank J. Fischer, R. Hardie, I. Hariharan, Y. Hiromi, E. O'Neill, R. Tjian, and C. Zuker for improving the manuscript with their comments. This work was supported by a National Science Foundation predoctoral fellowship to M.E.F. and by National Institutes of Health grant GM-33135 to G.M.R.

Note added in proof

Rhodopsin promoter sequence data described in this paper have been submitted to the EMBL/GenBank Data Libraries under accession numbers X51348 and X51353.

References

Ashburner, M., C. Detwiler, S. Tsubota, and R.C. Woodruff. 1983. The genetics of a small autosomal region of *Drosophila melanogaster* containing the structural gene for alcohol dehydrogenase. VI. Induced revertants of *Scutoid*. *Genetics* **104:** 405–431.

Autrum, H. and H. Stumpf. 1950. Das Bienenauge als Analysator für polarisiertes Licht. *Z. Naturforsch.* **5b:** 116–122.

Banerjee, U., P.J. Renfranz, J.A. Pollock, and S. Benzer. 1987. Molecular characterization and expression of *sevenless*, a gene involved in neuronal pattern formation in the *Drosophila* eye. *Cell* **49:** 281–291.

Biggin, M.D., S. Bickel, M. Benson, V. Pirotta, and R. Tjian. 1988. *Zeste* encodes a sequence-specific transcription factor that activates the *Ultrabithorax* promoter in vitro. *Cell* **53:** 713–722.

Bray, S.J., W.A. Johnson, J. Hirsh, U. Heberlein, and R. Tjian. 1988. A *cis*-acting element and associated binding factor required for CNS expression of the *Drosophila melanogaster* dopa decarboxylase gene. *EMBO J.* **7:** 177–188.

Courey, A.J., D.A. Holtzman, S.P. Jackson, and R. Tjian. 1989. Synergistic activation by the glutamine-rich domains of human transcription factor Sp1. *Cell* **59:** 827–836.

Dietrich, W. 1909. Die Facettenaugen der Dipteren. *Z. Wiss. Zool.* **92:** 465–539.

Dynan, W.S. 1989. Modularity in promoters and enhancers. *Cell* **58:** 1–4.

Fischbach, K.-F. 1979. Simultaneous and successive colour contrast expressed in 'slow' phototactic behaviour of walking *Drosophila melanogaster*. *J. Comp. Physiol.* **130:** 161–171.

Fischbach, K.-F. and A.P.M. Dittrich. 1989. The optic lobe of *Drosophila melanogaster*. I. A Golgi analysis of wild-type structure. *Cell Tissue Res.* **258:** 441–475.

Fischer, J.A. and T. Maniatis. 1988. *Drosophila Adh:* A promoter element expands the tissue specificity of an enhancer. *Cell* **53:** 451–461.

Fortini, M.E. 1990. Transcriptional regulation of R7 opsin genes in *Drosophila melanogaster*. Ph.D. thesis. University of California, Berkeley.

Franceschini, N. 1984. Chromatic organization and sexual dimorphism of the fly retinal mosaic. In *Photoreceptors* (ed. A. Borsellino and L. Cervetto), pp. 319–350. Plenum, New York.

Franceschini, N. and K. Kirschfeld. 1971a. Étude optique in vivo des éléments photorécepteurs dans l'oeil composé de *Drosophila*. *Kybernetik* **8:** 1–13.

———. 1971b. Les phénomènes de pseudopupille dans l'oeil composé de *Drosophila*. *Kybernetik* **9:** 159–182.

Franceschini, N., R.C. Hardie, W. Ribi, and K. Kirschfeld. 1981. Sexual dimorphism in a photoreceptor. *Nature* **291:** 241–244.

Fryxell, K.J. and E.M. Meyerowitz. 1987. An opsin gene that is expressed only in the R7 photoreceptor cell of *Drosophila*. *EMBO J.* **6:** 443–451.

Gorman, C.M., L.F. Moffat, and B.H. Howard. 1982. Recombinant genomes which express choloramphenicol acetyltransferase in mammalian cells. *Mol. Cell. Biol.* **2:** 1044–1051.

Hardie, R.C. 1984. Properties of photoreceptors R7 and R8 in dorsal marginal ommatidia in the compound eyes of *Musca* and *Calliphora*. *J. Comp. Physiol.* **154:** 157–165.

———. 1985. Functional organization of the fly retina. In *Progress in sensory physiology* (ed. D. Ottoson), vol 5, pp. 1–79. Springer-Verlag, Berlin.

———. 1986. The photoreceptor array of the dipteran retina. *Trends Neurosci.* **9:** 419–423.

Hardie, R.C., N. Franceschini, W. Ribi, and K. Kirschfeld. 1981. Distribution and properties of sex-specific photoreceptors in the fly *Musca domestica*. *J. Comp. Physiol.* **145:** 139–152.

Harris, W.A., W.S. Stark, and J.A. Walker. 1976. Genetic dissection of the photoreceptor system in the compound eye of *Drosophila melanogaster*. *J. Physiol.* (*London*) **256:** 415–439.

Hazelrigg, T., R. Levis, and G.M. Rubin. 1984. Transformation of *white* locus DNA in *Drosophila:* Dosage compensation, *zeste* interaction, and position effects. *Cell* **36:** 469–481.

Heisenberg, M. and E. Buchner. 1977. The rôle of retinula cell types in visual behavior of *Drosophila melanogaster*. *J. Comp. Physiol.* **117:** 127–162.

Heisenberg, M. and R. Wolf. 1984. Vision in *Drosophila:* Genetics of microbehavior. In *Studies of brain function* (ed. V. Braitenberg), vol. 12, pp. 1–32. Springer-Verlag, Berlin.

Hiromi, Y., A. Kuroiwa, and W.J. Gehring. 1985. Control elements of the *Drosophila* segmentation gene *fushi tarazu*.

Cell **43:** 603–613.

Hu, K.G., H. Reichert, and W.S. Stark. 1978. Electrophysiological characterization of *Drosophila* ocelli. *J. Comp. Physiol.* **126:** 15–24.

Kirschfeld, K., N. Franceschini, and B. Minke. 1977. Evidence for a sensitising pigment in fly photoreceptors. *Nature* **269:** 386–390.

Kirschfeld, K., R. Feiler, and N. Franceschini. 1978. A photostable pigment within the rhabdomere of fly photoreceptors no. 7. *J. Comp. Physiol.* **125:** 275–284.

Labhart, T. 1980. Specialized photoreceptors at the dorsal rim of the honeybee's compound eye: Polarizational and angular sensitivity. *J. Comp. Physiol.* **141:** 19–30.

Laski, F.A., D.C. Rio, and G.M. Rubin. 1986. Tissue specificity of *Drosophila* P element transposition is regulated at the level of mRNA splicing. *Cell* **44:** 7–19.

Levis, R., T. Hazelrigg, and G.M. Rubin. 1985. Effects of genomic position on the expression of transduced copies of the *white* gene of *Drosophila*. *Science* **229:** 558–561.

Lindsley, D.L. and E.H. Grell. 1968. Genetic variations of *Drosophila melanogaster*. *Carnegie Institute of Washington Publ.* No. 627.

Maniatis, T., E.F. Frisch, and J. Sambrook. 1982. *Molecular cloning: a laboratory manual*. Cold Spring Harbor Laboratory Press, Cold Spring Harbor, New York.

Marsh, J.L., M. Erfle, and E.J. Wykes. 1984. The pIC plasmid and phage vectors with versatile cloning sites for recombinant selection by insertional inactivation. *Gene* **32:** 481–485.

Menne, D. and H.C. Spatz. 1977. Color vision in *Drosophila melanogaster*. *J. Comp. Physiol.* **114:** 301–312.

Mismer, D. and G.M. Rubin. 1987. Analysis of the promoter of the *ninaE* opsin gene in *Drosophila melanogaster*. *Genetics* **116:** 565–578.

———. 1989. Definition of *cis*-acting elements regulating expression of the *Drosophila melanogaster ninaE* opsin gene by oligonucleotide-directed mutagenesis. *Genetics* **121:** 77–87.

Mismer, D., W.M. Michael, T.R. Laverty, and G.M. Rubin. 1988. Analysis of the promoter of the *Rh2* opsin gene in *Drosophila melanogaster*. *Genetics* **120:** 173–180.

Mitchell, P.J. and R. Tjian. 1989. Transcriptional regulation in mammalian cells by sequence-specific DNA binding proteins. *Science* **245:** 371–378.

Montell, C. and G.M. Rubin. 1988. The *Drosophila ninaC* locus encodes two photoreceptor cell specific proteins with domains homologous to protein kinases and the myosin heavy chain head. *Cell* **52:** 757–772.

———. 1989. Molecular characterization of the *Drosophila trp* locus: A putative integral membrane protein required for phototransduction. *Neuron* **2:** 1313–1323.

Montell, C., K. Jones, C. Zuker, and G.M. Rubin. 1987. A second opsin gene expressed in the ultraviolet-sensitive R7 photoreceptor cells of *Drosophila melanogaster*. *J. Neurosci.* **7:** 1558–1566.

Moses, K., M.C. Ellis, and G.M. Rubin. 1989. The *glass* gene encodes a zinc-finger protein required by *Drosophila* photoreceptor cells. *Nature* **340:** 531–536.

Müller, J., F. Thüringer, M. Biggin, B. Züst, and M. Bienz. 1989. Coordinate action of a proximal homeoprotein binding site and a distal sequence confers the *Ultrabithorax* expression pattern in the visceral mesoderm. *EMBO J.* **8:** 4143–4151.

Pollock, J.A. and S. Benzer. 1988. Transcript localization of four opsin genes in the three visual organs of *Drosophila*; *Rh2* is ocellus specific. *Nature* **333:** 779–782.

Ready, D.F. 1989. A multifaceted approach to neural development. *Trends Neurosci.* **12:** 102–110.

Ready, D.F., T.E. Hanson, and S. Benzer. 1976. Development of the *Drosophila* retina, a neurocrystalline lattice. *Dev. Biol.* **53:** 217–240.

Reinke, R. and S.L. Zipursky. 1988. Cell-cell interaction in the *Drosophila* retina: The *bride of sevenless* gene is required in photoreceptor cell R8 for R7 cell development. *Cell* **55:** 321–330.

Reinke, R., D.E. Kratz, D. Yen, and S.L. Zipursky. 1988. Chaoptin, a cell surface glycoprotein required for *Drosophila* photoreceptor cell morphogenesis, contains a repeat motif found in yeast and human. *Cell* **52:** 291–301.

Rogers, S.G. and B. Weiss. 1980. Exonuclease III of *Escherichia coli* K-12, an AP exonuclease. *Methods Enzymol.* **65:** 201–211.

Rubin, G.M. 1989. Development of the *Drosophila* retina: Inductive events studied at single cell resolution. *Cell* **57:** 519–520.

Rubin, G.M. and A.C. Spradling. 1982. Genetic transformation of *Drosophila* with transposable element vectors. *Science* **218:** 348–353.

Sanger, F., S. Nicklen, and A. R. Coulson. 1977. DNA sequencing with chain terminating inhibitors. *Proc. Natl. Acad. Sci.* **74:** 5463–5467.

Schmidt, B. 1975. Die neuronale Organisation in den Ocellen von *Drosophila*, Ph.D. thesis. University of Freiburg.

Schneuwly, S., R.D. Shortridge, D.C. Larrivee, T. Ono, M. Ozaki, and W.L. Pak. 1989. *Drosophila ninaA* gene encodes an eye-specific cyclophilin (cyclosporine A binding protein). *Proc. Natl. Acad. Sci.* **86:** 5390–5394.

Scholnick, S.B., S.J. Bray, B.A. Morgan, C.A. McCormick, and J. Hirsh. 1986. CNS and hypoderm regulatory elements of the *Drosophila melanogaster* dopa decarboxylase gene. *Science* **234:** 998–1002.

Schümperli, R.A. 1973. Evidence for colour vision in *Drosophila melanogaster* through spontaneous phototactic choice behaviour. *J. Comp. Physiol.* **86:** 77–94.

Seifert, H.S., E.Y. Chen, M. So, and F. Heffron. 1986. Shuttle mutagenesis: A method of transposon mutagenesis for *Saccharomyces cerevisiae*. *Proc. Natl. Acad. Sci.* **83:** 735–739.

Shieh, B.-H., M.A. Stamnes, S. Seavello, G.L. Harris, and C.S. Zuker. 1989. The *ninaA* gene required for visual transduction in *Drosophila* encodes a homologue of cyclosporin A-binding protein. *Nature* **338:** 67–70.

Smith, D., B.-H. Shieh, and C.S. Zuker. 1990. Isolation and structure of an arrestin gene from *Drosophila*. *Proc. Natl. Acad. Sci.* (in press).

Smola, U. and P. Meffert. 1979. The spectral sensitivity of the visual cells R7 and R8 in the eye of the blowfly *Calliphora erythrocephala*. *J. Comp. Physiol.* **133:** 41–52.

Spradling, A.C. and G.M. Rubin. 1982. Transposition of cloned P elements into *Drosophila* germ line chromosomes. *Science* **218:** 341–347.

———. 1983. The effect of chromosomal position on the expression of the *Drosophila* xanthine dehydrogenase gene. *Cell* **34:** 47–57.

Stark, W.S., R. Sapp, and S.D. Carlson. 1989. Ultrastructure of the ocellar visual system in normal and mutant *Drosophila melanogaster*. *J. Neurogenet.* **5:** 127–153.

Stephens, G.C., M. Fingerman, and F.A. Brown. 1953. The orientation of *Drosophila* to plane polarized light. *Ann. Entomol. Soc. Am.* **46:** 75–83.

Strausfeld, N. and H. Wunderer. 1985. Optic lobe projections of marginal ommatidia in *Calliphora erythrocephala* specialized for detecting polarized light. *Cell Tissue Res.* **242:** 163–178.

Tomlinson, A. 1988. Cellular interactions in the developing *Drosophila* eye. *Development* **104:** 183–193.

Treisman, R. and T. Maniatis. 1985. Simian virus 40 enhancer increases number of RNA polymerase II molecules on linked DNA. *Nature* **315:** 72–75.

Wada, S. 1971. Ein spezieller Rhabdomerentyp im Fliegenauge. *Experientia* **27:** 1237–1238.

———. 1974. Spezielle randzonale Ommatidien der Fliegen (Diptera: Brachycera): Architektur und Verteilung in den Komplexaugen. *Z. Morph. Tiere* **77:** 87–125.

Wehner, R. 1982. Himmelsnavigation bei Insekten. Neurophysiologie und Verhalten. In *Neujahrsblatt der naturforschenden Gesellschaft in Zürich* (ed. H.H. Bossard). Naturforschende Gesellschaft, Zürich. **184**.

———. 1989. Neurobiology of polarization vision. *Trends Neurosci.* **12:** 353–359.

Wolf, R., B. Gebhardt, R. Gademann, and M. Heisenberg. 1980. Polarization sensitivity of course control in *Drosophila melanogaster*. *J. Comp. Physiol.* **139:** 177–191.

Wong, F., E.L. Schaefer, B.C. Roop, J.N. LaMendola, D. Johnson-Seaton, and D. Shao. 1989. Proper function of the *Drosophila trp* gene product during pupal development is important for normal visual transduction in the adult. *Neuron* **3:** 81–94.

Wunderer, H. and U. Smola. 1982a. Morphological differentiation of the central visual cells R7/8 in various regions of the blowfly eye. *Tissue Cell* **14:** 341–358.

———. 1982b. Fine structure of ommatidia at the dorsal eye margin of *Calliphora erythrocephala* Meigen (Diptera: Calliphoridae). An eye region specialized for the detection of polarized light. *Int. J. Insect Morphol. Embryol.* **11:** 25–38.

Zipursky, S.L. 1989. Molecular and genetic analysis of *Drosophila* eye development: *sevenless*, *bride of sevenless* and *rough*. *Trends Neurosci.* **12:** 183–189.

Zuker, C.S., C. Montell, K. Jones, T. Laverty, and G.M. Rubin. 1987. A rhodopsin gene expressed in photoreceptor cell R7 of the *Drosophila* eye: Homologies with other signal-transducing molecules. *J. Neurosci.* **7:** 1550–1557.